# Ocean Acidification Responses in Paralarval Squid Swimming Behavior Using a Novel 3D Tracking System

Casey Zakroff[1,2,3], T. Aran Mooney[2], Colin Wirth[2]

Corresponding Author: Casey Zakroff, czakroff@whoi.edu, ORCID: 0000-0001-6979-1857

[1]Massachusetts Institute of Technology-Woods Hole Oceanographic Institution Joint Program in Oceanography/Applied Ocean Science and Engineering, Cambridge, MA, USA

[2]Biology Department, Woods Hole Oceanographic Institution, Woods Hole, MA, USA

[3]Red Sea Research Center, King Abdullah University of Science and Technology, Thuwal, 23955-6900, Saudi Arabia

Keywords: hypercapnia, cephalopod, larvae, movement analysis, stress physiology

**Acknowledgments**

We thank D. Remsen, the MBL Marine Resources Center staff, and MBL *Gemma* crew for their support in acquiring squid. R. Galat and the facilities staff of the WHOI ESL provided system support. D. McCorkle, KYK Chan, and M. White provided valuable insight on the OA system. E. Moberg, A. Beet, and A. Solow assisted in the development and coding of the 3D model system. We also thank E. Bonk, K. Hoering, M. Lee, D. Weiler, and A. Schlunk for their assistance and input with the experiments. This material is based upon work supported by the National Science Foundation Graduate Research Fellowship under Grant No. 1122374. This project is funded by NSF Grant No. 1220034.

**Abstract**

Chronic embryonic exposure to ocean acidification (OA) has been shown to degrade the aragonitic statolith of paralarval squid, *Doryteuthis pealeii*, a key structure for their swimming behavior. This study examined if day-of-hatching paralarval *D. pealeii* from eggs reared under chronic OA demonstrated measurable impairments to swimming activity and control. This required the development of a novel, cost-effective, and robust method for 3D motion tracking and analysis. Squid eggs were reared in $pCO_2$ levels in a dose-dependent manner ranging from 400 - 2200 ppm. Initial 2D experiments showed paralarvae in higher acidification environments spent more time at depth. In 3D experiments, velocity, particularly positive and negative vertical velocities, significantly decreased from 400 to 1000 ppm $pCO_2$, but showed non-significant decreases at higher concentrations. Activity and horizontal velocity decreased linearly with increasing $pCO_2$, indicating a subtle impact to paralarval energetics. Patterns may have been obscured by notable individual variability in the paralarvae. Responses were also seen to vary between trials on cohort or potentially annual scales. Overall, paralarval swimming appeared resilient to OA, with effects being slight. The newly developed 3D tracking system provides a powerful and accessible method for future studies to explore similar questions in the larvae of aquatic taxa.

This is a post-peer-review, pre-copyedit version of an article published in Hydrobiologia. The final authenticated version is available online at: http://dx.doi.org/10.1007/s10750-017-3342-9

## Introduction

Ocean acidification (OA) has emerged as a prominent threat to marine systems, with rising atmospheric $CO_2$ concentrations decreasing ocean pH at rates unparalleled in geologic history (Doney et al., 2009; Honisch et al., 2012). Coastal systems are particularly susceptible due to freshwater influx and concurrent anthropogenic impacts, e.g. eutrophication, reducing the buffering capacity and increasing the pH variability of these waters (Gledhill et al., 2015). Nearshore marine systems provide nursery habitat to a range of ecological and economically vital species, including the longfin inshore squid, *Doryteuthis pealeii*, a keystone species in the Northwest Atlantic coastal trophic web and a substantial fishery (Macy III, 1982; Beck et al., 2001; Jacobson, 2005; Hunsicker & Essington, 2008). This member of the demersal Lolignid squids is a seasonal migrator, overwintering on the continental shelf and breeding nearshore south of the Mid-Atlantic Bight, before coming north and inshore to areas like Vineyard Sound, MA, USA from late spring through early autumn for peak breeding season (Macy III & Brodziak, 2001; Jacobson, 2005). The squid leave mops of egg capsules tied to the seafloor, each containing embryos, 50 - 200 per capsule, which must develop under whatever conditions they are laid in, enduring environmental stress until hatching (Arnold et al., 1974; Jacobson, 2005). At hatching, the paralarvae must cope both with the shock of the transition into a neritic, planktonic phase and the continued stress of their environment until they are transported by prevailing currents (Robin et al., 2014). Paralarval survivorship is naturally low, with greatest mortality occurring during the no net growth, post-hatch period while transitioning from yolk reserves to exogenous feeding (Vidal et al., 2002a; Robin et al., 2014). Sublethal physiological changes to embryonic condition, metabolism, or sensory systems imposed by environmental stressors, such as OA, could express as shifts in hatchling paralarval swimming activity and behavior. Any

This is a post-peer-review, pre-copyedit version of an article published in Hydrobiologia. The final authenticated version is available online at: http://dx.doi.org/10.1007/s10750-017-3342-9

impairments arising during this sensitive transitional phase could be detrimental not only to individual squid success, but also to overall population structure (Byrne, 2011; Robin et al., 2014).

Swimming is key to paralarval squid survival; the mantle fins are rudimentary post-hatch, therefore hatchlings rely primarily on jetting for motion, which is necessary in capturing prey and avoiding predators (Vecchione, 1981). Paralarvae operate at intermediate Reynolds numbers (25 - 90), balancing between the viscous world at low speeds and a more inertial world during their high speed jets (Bartol et al., 2009a). They are also negatively buoyant: slowly, passively sinking before jetting upwards in bursts, displaying a characteristic 'hop and sink' pattern, which is believed to conserve energy (Haury & Weihs, 1976; Staaf et al., 2014). Jetting is an energetically costly means of motion, but one that provides remarkable propulsive efficiency at the paralarval stage (Bartol et al., 2008, 2009b). During the post-hatch transitional phase, paralarvae must operate with a finite fuel reserve, the yolk, to power their jets as they avoid predation and learn to predate, but this same energy source is also tapped to mitigate stress and maintain homeostasis (Vidal et al., 2002a; Sokolova et al., 2012).

Under natural conditions, the fluid surrounding the chorions of *D. pealeii* embryos within an egg capsule reaches dramatically low pH (7.34) and oxygen concentrations (1.9 μmol $l^{-1}$) prior to hatching: a potentially taxing physiological state that may be exacerbated by ocean acidification (Long et al., 2016). Both hypercapnia and decreased pH can elicit metabolic depression in marine ectotherms, a common stress coping response (Guppy & Withers, 1999; Sokolova, 2013). Depression of oxygen consumption rate has been shown to occur in the embryos and hatchling paralarvae of high-$CO_2$ exposed eggs of the European squid, *Loligo vulgaris* (Rosa et al., 2014). Cephalopods have substantial homeostatic machinery, energy-

This is a post-peer-review, pre-copyedit version of an article published in Hydrobiologia. The final authenticated version is available online at: http://dx.doi.org/10.1007/s10750-017-3342-9

93 dependent acid-base transporters, with which they can maintain extracellular pH (Gutowska et
94 al., 2010). They may be capable, then, of reallocating energy across active biological processes,
95 in order to retain their overall metabolic rate (Sokolova et al., 2012). Reduced dorsal mantle
96 length (DML) and increased embryonic development time have been seen in *D. pealeii*
97 hatchlings exposed to chronic OA, which may be indicative of such a homeostatic response
98 (Kaplan et al., 2013). Both metabolic depression and energy budget reallocation during
99 embryonic development could result in a subsequent reduction in hatchling paralarvae swimming
100 activity or speed.

101 The statoliths (small aragonitic stones connected to sensory hair cells) are the core
102 sensory structures for control of motion balance, and orientation in the cephalopods (Messenger,
103 1970; Arkhipkin & Bizikov, 2000). Absence of the paralarval statolith resulting from a lack of
104 strontium in artificial seawater has been shown to cause aberrant "spinning" behaviors in several
105 cephalopod taxa (Hanlon et al., 1989). *D. pealeii* paralarvae have demonstrated a reduction in
106 statolith size and quality after exposure to high levels of $CO_2$ during development (Kaplan et al.,
107 2013). This present study sought to repeat and expand on the above mentioned study by
108 recording and tracking the movement of squid paralarvae in order to examine if chronic
109 embryonic exposure to OA caused impairments to their general swimming activity and
110 orientation ability.

111 Squid paralarvae present a distinct challenge in larval tracking with current
112 methodologies. As small (approximate DML of 1.8 mm, total length of 3 mm), translucent
113 organisms, squid paralarvae are well-suited to digital particle image velocimetry (DPIV) studies
114 (Bartol et al., 2008, 2009a, 2009b). These studies, while advantageous for dissecting the
115 mechanics of motion and flow in many taxa, are primarily done in two-dimensions (2D) as the

116 set up and equipment, and subsequent costs associated with requiring both a laser and high-speed
117 camera, are substantial (Stamhuis & Videler, 1995; Fuchs et al., 2004; Wheeler et al., 2013).
118 Early techniques of larval videography and tracking were enacted in simple, cost-
119 effective 2D systems, such as petri dishes or round aquariums, where the animal was recorded in
120 the horizontal *x*, *y* plane from a camera directly above (Wassersug & von Seckendorf Hoff, 1985;
121 Villanueva et al., 1997; Budick & O'Malley, 2000). These systems were limiting for a study with
122 squid paralarvae given the dominance of vertical motions in their swimming behavior (Staaf et
123 al., 2014). Stereoscopic camera systems are commonly used in the field to detect accurate depth
124 and positional information of oceanic organisms (Klimley & Brown, 1983; Boisclair, 1992). In
125 lab, this method requires lighting from the front, however, which can alter the behavior of
126 positively phototactic organisms like squid.
127 Using two perpendicular cameras allows for unbiased lighting while still capturing the
128 organism in all three dimensions. Such methods can produce a clear movement track, but often
129 require specially designed systems, either with motorized camera set ups or with uniquely shaped
130 aquaria that limit movement range in the *y* axis (Coughlin et al., 1992; Cachat et al., 2011a,
131 2011b). We found we were limited by existing tracking software being both prohibitively
132 expensive and, in testing, proving not to successfully function in tracking videos of the squid
133 paralarvae. In order to observe swimming at the resolution and accuracy needed to examine our
134 OA-driven questions, we had a clear need to develop a method of three-dimensional (3D)
135 analysis that would not limit or coerce the motion of the organism and would produce clear,
136 well-lit video wherein the organism could be tracked effectively by readily available software.
137 The aim of this study was to evaluate the potential effects of ocean acidification on post-
138 hatch paralarval squid*, D. pealeii,* swimming behavior using newly-hatched paralarvae reared

under a range of $CO_2$ concentrations (and thus a range of pH treatments). Across their range, and dependent on season, adult *D. pealeii* can be found in depths ranging from 1 - 400 m, temperatures ranging from 4 - 28 ºC, and salinities ranging from 30-37 ppt. Juvenile and adult *D. pealeii* have been found in the Hudson-Raritan estuary, a system with much greater temperature, salinity, and pH variation than the coastal shelf, which may indicate these life stages are capable of at least acute exposure to a wide range of environmental conditions (Jacobson, 2005). Comprehensive measurements of in situ environmental pH in *D.* pealeii habitat across its range have not been performed to our knowledge, but ranges of mean shelf $pH_{total}(20)$ of 7.85 - 8.05 and $fCO_2(20)$ of 400 - 700 ppm were reported from North Carolina to New Hampshire from a coastal carbon cruise conducted in summer (July/August) (Wang et al., 2013). Little is documented about the ecology or environmental exposures of the paralarval life phase of squid, but rearing experiments with Loliginids indicate high water quality and a recommended pH > 8.0 are best for their survival (Hanlon et al., 1983; Vidal et al., 2002b).

Our study focused on specimens from and comparisons to the Vineyard Sound, MA system where *D. pealeii* eggs are laid every summer. This work encompassed a range of $CO_2$ levels between current ambient (400 ppm) and the elevated treatment used in Kaplan et al. (2013). The high treatment, 2200 ppm, is predicted for 2300 based on IPCC IS92a, but is naturally found in the very extreme inshore estuary conditions of Vineyard sound (Caldeira & Wickett, 2003; McCorkle et al., 2012). The intent was to examine the physiological scope and sensitivity of hatchling paralarval swimming. We hypothesized, based on initial work by Kaplan et al. (2013), that activity levels, speed, and control of orientation would be impaired in OA-exposed paralarvae due to impairments to their physiological and sensory systems. The question posed required a robust visualization of the energetics and kinematics of paralarval swimming,

This is a post-peer-review, pre-copyedit version of an article published in Hydrobiologia. The final authenticated version is available online at: http://dx.doi.org/10.1007/s10750-017-3342-9

which required the development of a novel, simple, and feasible method of 3D paralarval tracking and analysis that we present here alongside the experimental data.

## Materials and Methods

### *Squid Collection and Husbandry*

Experiments were conducted at the Environmental Systems Laboratory (ESL) at the Woods Hole Oceanographic Institution, Woods Hole, MA, USA from June-August 2013, May-October 2014, and May-June 2015. This timing corresponds with the peak breeding season of the Atlantic Longfin squid, *Doryteuthis pealeii*, in the nearshore of New England (Jacobson, 2005). Although the full breadth and physical properties of *D. pealeii* egg habitat is not well described, eggs in New England waters are typically found at depths less than 50 m, with temperature and salinity ranges of 10 - 23 ºC, and 30 - 32 ppt, respectively (McMahon & Summers, 1971; Jacobson, 2005; Shashar & Hanlon, 2013). Squid were collected during trawls in Vineyard Sound at 10-30 meters depth by the Marine Biological Laboratory (MBL). Sea surface temperatures in Vineyard Sound, MA, USA ranged from 8.4 - 25.8 ºC with a mean of 19.4 ºC from May - October (compiled for 2013 - 2015 from NOAA Station BZBM3). Bottle samples (n = 5) were taken in Vineyard Sound at 20 m depth (processed for Alk/DIC using VINDTA) in the morning once every two weeks from late July - late September 2014 off of the MBL squid trawler at the site of capture, along with accompanying CTD casts (CastAway CTD, SonTek, San Diego, USA). These data show a temperature range of 17.4 - 19.6 ºC, salinity range of 31.3-32.5 psu, total alkalinity range of 2148.1 - 2195.2 µmol / kg, DIC range of 1962.7 - 2038.2 µmol / kg, $pH_{total}$ range of 7.96 - 8.00, and $pCO_2$ range of 439.9 - 486.5 ppm, but are limited in scope in reference to the whole breeding season.

This is a post-peer-review, pre-copyedit version of an article published in Hydrobiologia. The final authenticated version is available online at: http://dx.doi.org/10.1007/s10750-017-3342-9

Intact, adult squid (mid-sized, 20-25 cm DML without fin tears/skin lesions) were hand-selected from the trawl catch at the MBL's Marine Resources Center dock. Individuals were gently placed in seawater-filled coolers and transported by car to the ESL immediately after the ship's return (< 6 hours post-capture), and transferred to the ESL holding aquaria. All transport activity was performed as carefully and expediently as possible to minimize stress to the breeding adults, but overall capture and transit stress was unavoidable. Eighteen squid were selected for breeding; reproductively active females (differentiated by their bright orange accessory nidamental gland) and males, displaying visible and dense sperm packets, were selected in a 2:1 female:male ratio to enhance breeding probability.

Upon arrival at the ESL, squid were split equally between two holding tanks (120 cm diameter, 70 cm depth), maintaining the 2:1 gender ratio. Holding tanks were flow-through, using water pumped directly from Vineyard Sound (approximately 100 yards offshore of the ESL) that had been sand-filtered and cooled to 15°C (Salinity = 33 psu, $pH_{nbs}$ = 7.96), and continuously bubbled with air. This temperature was within the range naturally experienced by the adults during the breeding season and reduced thermal and metabolic stress on the adults, as well as the incidence of infighting and cannibalism, compared to if they were housed at ambient temperatures. Squid were fed once per day with locally captured killifish, *Fundulus heteroclitus*, gathered from Salt Pond, Woods Hole, MA. Upon discovery, mops of egg capsules were transferred into a bucket of water from the adult tank and carried to the room containing the ocean acidification system where they were hand sorted into the experimental cups. Only good quality egg capsules, those that were long and finger-like with an orange tinge and laid in neat mops, were chosen; egg capsules contained between 90 - 300 eggs, which is expected for this

207 species (Arnold et al., 1974; Maxwell & Hanlon, 2000). Adult squid were maintained in the
208 tanks at the ESL until they died following breeding.
209
210 *Ocean Acidification System*
211 In brief, for each trial, *D. pealeii* egg capsules collected from the squid aquaria were
212 randomly sorted into flow-through cups (1-liter PET food service containers [Solo Foodservice,
213 Lake Forest, IL]) filled with seawater delivered via drip lines from upstream equilibration
214 chambers. These chambers were bubbled with $CO_2$ and air to maintain respective $CO_2$
215 concentrations (ranging from 400 ppm to 2200 ppm). All rearing cups were contained within a
216 20ºC water bath under a 14:10 hour light:dark cycle. No temperature acclimation was conducted
217 for the eggs, as this level of temperature shift did not appear to notably impact embryonic
218 development or survival, or paralarval viability. This temperature and light regime approximated
219 the average values in Vineyard Sound (19.4 ºC) across the breeding season, late April to early
220 October. A rearing temperature of 20 ºC was chosen as it reflected natural conditions, to replicate
221 the conditions in the previous work by Kaplan et al. (2013), and because temperature controls the
222 development time of *D. pealeii,* and so resulted in a consistent 14 day time to hatching at the
223 control $pCO_2$ (McMahon & Summers, 1971; Zeidberg et al., 2011). There were three cups
224 containing two egg capsules each and one chemical control cup per treatment per trial. Flow
225 rates to the cups were approximately 20 l $day^{-1}$, which prevented waste accumulation. Water
226 quality of the experimental cups was monitored using a pH probe (Orion Star™ A329, Thermo
227 Fisher Scientific Inc., Waltham, MA, USA) every three days, while alkalinity, salinity, and
228 spectrometric pH readings were taken weekly in order to calculate $pCO_2$ with CO2SYS (Table 1)

(a full OA system description, experimental procedure, and $CO_2$ monitoring methods can be found in the Electronic Supplementary Material).

*Paralarvae Sampling*

Squid embryos were allowed to develop undisturbed in the OA system. Upon hatching, paralarvae from each cup were subsampled for a range of experiments, including behavioral videography. At the end of each hatching day, all paralarvae were removed from the system and preserved (anesthetized with 7.5 % w/v $MgCl_2$ mixed with equal part seawater and preserved in 70% ethanol) ensuring that all hatchlings used were less than 24 hours old. Over the first 3 - 6 days of hatching, 10 - 20 individual paralarvae per cup per treatment were collected for behavioral videos, in order to obtain multiple analyzable videos per treatment per trial. Paralarvae were haphazardly selected from the cups, avoiding those that exhibited a constant spinning behavior, which has been described both as an aberrant effect of aquarium-rearing and as a potential stereotyped predator defense (Hanlon et al., 1989; York & Bartol, 2016). Tests in 2013 demonstrated there was no difference in this behavior across $CO_2$ treatments (ANOVA, $F_{5, 21} = 2.31$, $p = 0.0805$). As there was only one arena/camera set up, videography was done for one experimental cup at a time. Per each cup, the arena was filled with water from the control cup for that treatment. Individual paralarvae (n = 10 - 15) from the experimental cup were transferred using a plastic pipet and kept within a 24 well plate (Falcon® Brand 2.0 $cm^2$ well area, 3.5 mL well volume, Corning Inc., Corning, NY, USA) filled with water from the same cup, one paralarva per well, until filming occurred. A filming period for one cup took at most an hour ([1 minute acclimation + 2 minutes recording + 1 minute removal and reset] * 10 - 15 paralarvae = 40 - 60 minutes per cup). It was assumed, although not tested, that water quality in the well plate

and arena was that of the experimental treatment sampled and did not notably change over the brief filming period. The arena and well plate were refilled for each filming period and treatments were selected from in a rotation, so as to not bias sampling by time of day. Overall more videos were recorded than were analyzed in both the 2D and 3D systems for all analyses, as only videos where the paralarvae was visible, away from the corners, exhibiting normal swimming/responses, and, in the case of the 3D metrics, trackable could be used (Table 1)

*Swimming Behavior Experiments*

Over the course of developing a viable 3D system, two different arenas were used resulting in two separate swimming behavior experiments. Experiment 1 consisted of Trials 1, 2 and 4 of 2013 and Trial 1 of 2014 (Table 1). Trials were run in a tall, rectangular arena that constrained movement in the *y* axis, but only 2D vertical swimming data could be tracked and analyzed from this system. Implemented in Experiment 2 (Trials 2, 3, and 4 in 2014 and in Trial 1 of 2015; Table 1), the cubic arena and model system allowed for full 3D tracking and analysis.

Wall effects were considered for both experiments, however the viscous effects of walls at low Reynolds numbers should not impact paralarvae given their size and speed (Vogel, 1981). Damage caused by wall impacts is a common source of mortality among aquarium housed squid, and it is best to make the walls visible to help avoid this, however this would have obscured recording and lighting (Summers et al., 1974). Many paralarvae interacted with the walls during recordings, but this did not appear to cause harm or behavioral shifts, although paralarvae were not subsequently checked for dermal abrasions. Increasing the available swimming volume from the 2D to the 3D arena was intended to reduce potential arena effects, although overall arena size was limited by available space (e.g. camera viewing scope within the covered light box).

This is a post-peer-review, pre-copyedit version of an article published in Hydrobiologia. The final authenticated version is available online at: http://dx.doi.org/10.1007/s10750-017-3342-9

In order to determine acclimation time, 10-minute recordings of individual paralarvae (9 useable videos analyzed of 20 videos taken), sampled from all treatments, placed into the arena were conducted. Paralarval activity, described by jetting or active mantle pulsation, showed no significant differences across 1-minute bins of the ten-minute observation period (Kruskal-Wallis, $p = 0.9284$). We do not claim that the paralarvae became accustomed to the arena, however there were no significant changes to their behavior within a reasonable recording timeframe (Supplementary Materials, Fig. S1). An acclimation time of 1 minute was therefore used for both experiments, in order to maximize the sample size of videos taken (Table 1).

*Experiment 1: 2D Swimming Behavior*

The trials of the first experiment took place during the summer of 2013 and in May of 2014. Experiment 1 used a preliminary 2D filming arena constructed from 500 mL tissue culture flasks (Corning Inc., Corning, NY, USA) by removing the top, capped portion, creating a standing container with internal dimensions of 10.6 cm width, 3.2 cm depth, and 14.0 cm height (*x*, *y*, and *z* axes) (Fig. S2a). All plastic containers were soaked for 24 hours in seawater and DI-water rinsed prior to use. Black card stock was attached to the back of the arena for contrast between the translucent organism and the background, allowing for better paralarval tracking. 400 mL of water from the corresponding $CO_2$ level was added to the chamber, corresponding to a 10.5 cm x 3.2 cm x 11.4 cm (*x*, *y*, and *z*) volume. This provided a large area, compared to the organism's size (approximately 3 mm), in the *x* and *z* axes while constraining movement in the *y* axis. This chamber was placed within a photobox (76.2 $cm^3$, B&H Foto & Electronics Corp, NY), which was covered with black tarp to block ambient light. Two LED panels with diffuser plates were placed on either side of the chamber to create equal lighting from both directions.

This is a post-peer-review, pre-copyedit version of an article published in Hydrobiologia. The final authenticated version is available online at: http://dx.doi.org/10.1007/s10750-017-3342-9

298 The strong photopositive response by paralarvae required lights be placed precisely and set to
299 equal intensities to exclude directional bias. Two HD video cameras were placed inside the
300 photobox at a 90º angle to the experimental chamber, one above (Sony HDR-XR550V) fastened
301 to a wooden frame and one in front (Sony HDR-CX 580V). Only information from the front
302 camera was used in later analyses due to poor larval visibility for tracking in footage from the
303 top-mounted camera. Videos were recorded at 29.97 frames per second.
304 For each video, an individual paralarva was pipetted from the tray directly into the center
305 of the chamber. After the one-minute acclimation period, swimming behavior was recorded for
306 one minute. Paralarvae were removed from the chamber using a pipet and were anesthetized with
307 7.5 % w/v $MgCl_2$ mixed with equal part seawater before being preserved in 70% ethanol.
308
309 *Experiment 1 Data Analysis*
310 Individual paralarvae videos were tracked using Tracker, marking the eyes of the
311 paralarvae, which were the most distinct and trackable feature (Open Source Physics,
312 comPADRE Digital Library). Variability in the 2D system's video quality, due to issues of light
313 reflection and clarity, and individual paralarval trackability (many paralarvae stayed near the
314 walls, entrained in the meniscus, or expressed the aforementioned spinning behaviors, which
315 made videos unusable) resulted in uneven sampling amongst the 2D data (total n = 394, Table 1).
316 Organisms were tracked using the autotracker function when video quality allowed this for
317 capability, but this function was corrected with manual tracking as needed. Positional data ($x$ & $z$
318 coordinates) were produced for each frame within the 60-second interval, totaling 1799 points
319 per recording. The $z$ axis of the arena was divided into equal thirds of 4.73 cm and positional
320 data were sorted into these depth bins for the top, middle, and bottom of the container using

This is a post-peer-review, pre-copyedit version of an article published in Hydrobiologia. The final authenticated version is available online at: http://dx.doi.org/10.1007/s10750-017-3342-9

Excel (Excel for Mac 2011, Microsoft Corp., Redmond, WA, USA). The number of frames per bin, directly proportional to time spent in each depth section, was calculated for each individual and compared across $CO_2$ treatment groups.

*Experiment 2: 3D Swimming Behavior*

The trials of the primary experiment using the developed 3D analysis system took place in the summer of 2014 and May of 2015. The recording arena for the 3D filming consisted of the bottom portion of a plastic display box (10.2 cm x 10.2 cm x 18.4 cm, Amac Plastic Products Corp., Petaluma, CA, USA) (Fig. S2b). Black card stock was attached to the back of the container in the *x*, *z* plane and black cotton cloth laid on the bottom of the container in the *x*, *y* plane, again to contrast translucent paralarvae. In the 2D arena, excessive light reflection could obscure paralarvae near the walls and a strong meniscus could entrain paralarvae to the surficial corners, but the greater area, and increased wall clarity of the 3D arena prevented these issues.

The 3D filming arena was set up in the same manner as the 2D arena within the photobox. The camera lenses were each aligned to the centroid of the chamber for their respective viewing planes (Fig. 1, A & B). Each camera was connected to its own monitor outside of the photobox so that paralarval swimming could be observed during the trials.

The chamber bottom measured 92.16 $cm^2$ inside (9.6 cm x 9.6 cm); therefore, the chamber was filled to 9.6 cm depth with water of the appropriate $CO_2$ concentration to create an 884.7 $cm^3$ cube to contain the organism (the model system requires a cubic water volume, as outlined below, but the size can be changed). Individual paralarvae were pipetted from a holding tray directly into the center of the filming arena and allowed to acclimate for one minute. Swimming behavior was then recorded for two minutes; increased from the previous 2D

This is a post-peer-review, pre-copyedit version of an article published in Hydrobiologia. The final authenticated version is available online at: http://dx.doi.org/10.1007/s10750-017-3342-9

344 experiments due to the improved video quality and tracking output of the 3D system as well as
345 the need for more path data for the more complex 3D metrics. The two minute period was
346 concluded by flashing a laser pointer into the filming chamber, which provided a synchronization
347 point for the top and side videos. Paralarvae were then removed from the chamber, anesthetized,
348 and preserved in 70% ethanol.
349
350 *Experiment 2 Data Analysis*
351 Videos from the top and side cameras were synched using the laser flash and cut to two-
352 minute clips for each paralarva. Videos were tracked using Tracker, using the eyes of the
353 paralarvae as the tracking feature, as with the 2D experiment. Although the 3D arena did not
354 diminish video quality as the 2D arena did, a large number of videos could still not be used, due
355 to paralarvae staying at walls and corners, or spinning (total tracked video n = 157, Table 1).
356 Positional data were produced for each frame in both viewing planes, resulting in 3,598 points
357 for each recording plane ($x$, $z$) and ($x$, $y$). Tracker functioned with the origin point for the
358 calibrating axes being set based on the orientation of the camera. Thus prior to correction for 3D,
359 the positional data were all transformed into the same 0, 0, 0 axes frame set at the bottom left
360 corner of the front plane of the filming arena using Excel.
361 To merge the two separate 2D positional datasets into a 3D dataset, the filming arena was
362 modeled as two series of diminishing planes, “side” and “top” (Fig. 1, C & D). In any given
363 video frame, the front plane of the chamber had the true dimensions of the arena, 92.16 $cm^2$.
364 Along the axis perpendicular to the axes of the video frame, the planes diminish in the image due
365 to the vanishing point effect, up unto the back of the arena. The value of the length of the side of
366 the cube was known ($Q$ = 9.6 cm). The organism was in some plane along the perpendicular axis,

This is a post-peer-review, pre-copyedit version of an article published in Hydrobiologia. The final authenticated version is available online at: http://dx.doi.org/10.1007/s10750-017-3342-9

so its position within its plane in the image is proportional to its true position in a 9.6 cm-sided square, such that

$$\frac{Q_s}{Q} = \frac{x_{is}}{x} \quad (1)$$

$$\frac{Q_s}{Q} = \frac{z_{is}}{z} \quad (2)$$

$$\frac{Q_t}{Q} = \frac{x_{it}}{x} \quad (3)$$

$$\frac{Q_t}{Q} = \frac{y_{it}}{y} \quad (4)$$

where $Q_s$ and $Q_t$ are the lengths of the plane the organism is in within the image and $x_{is}$, $z_{is}$, $x_{it}$ and $y_{it}$ are the positional coordinates of the organism within that plane, in the side and top, respectively.

The positional values of the organism were measureable within the coordinate axes of the front plane using Tracker: $x_s$ and $z_s$ for the side, and $x_t$ and $y_t$ for the top. The positional values of the organism in its image plane were modeled as the difference between these measured coordinates and the side of the right triangle formed between the front plane and the organism's image plane (Fig. 1, C & D):

$$x_{is} = x_s - q_{is}/\sqrt{2} \quad (5)$$

$$z_{is} = z_s - q_{is}/\sqrt{2} \quad (6)$$

$$x_{it} = x_t - q_{it}/\sqrt{2} \quad (7)$$

$$y_{it} = y_t - q_{it}/\sqrt{2} \quad (8)$$

where $q_{is}$ and $q_{it}$ are the hypotenuse of the right triangles for the side and top, respectively. The hypotenuse divided by the square root of two provides a measure of distance between the front

This is a post-peer-review, pre-copyedit version of an article published in Hydrobiologia. The final authenticated version is available online at: http://dx.doi.org/10.1007/s10750-017-3342-9

plane and the organism's image plane. It follows then that $Q_s$ and $Q_t$ are different to $Q$ by twice this measure:

9) $$Q_s = Q - 2 * \left(q_{is}/\sqrt{2}\right)$$

10) $$Q_t = Q - 2 * \left(q_{it}/\sqrt{2}\right)$$

The length of the side of the backmost plane was measureable within the film image for both the side and top camera ($q_{bs}$ and $q_{bt}$, respectively). The ratios between these values and the length of the filming arena are equal to the ratios between the distances between planes, $q_{is}$ and $q_{it}$, and the true distance of the image plane along the perpendicular axis, y and z, respectively:

11) $$\frac{q_{bs}}{Q} = \frac{q_{is}}{y}$$

12) $$\frac{q_{bt}}{Q} = \frac{q_{it}}{z}$$

This results in an over-constrained system. Datasets for individual paralarva with all measured values were run through a MATLAB (R2016b, MathWorks, Inc., Natick, MA, USA) custom-built script (in the Electronic Supplementary Material and at https://github.com/czakroff/3D-Swimming-Behavior) which calculated the *x*, *y*, and *z* values for the system by using least sum of squares to determine the values for each frame that result in the least error. These data were then run in a separate MATLAB custom-built script (in the Electronic Supplementary Material and at https://github.com/czakroff/3D-Swimming-Behavior) to visualize paralarval swimming tracks and calculate a range of 3D metrics, including total distance traveled (cm), 3D velocity (cm $s^{-1}$), vertical and horizontal velocities (cm $s^{-1}$), and volume ($cm^3$) transited for each individual paralarva. All video measurements were taken and all subsequent analyses using the model system and codes were run using centimeters. However, all results have been shifted into millimeters for better readability in publication. 3D metrics were

This is a post-peer-review, pre-copyedit version of an article published in Hydrobiologia. The final authenticated version is available online at: http://dx.doi.org/10.1007/s10750-017-3342-9

409 further analyzed in ten-second time bins across the 120-second recording period for each
410 individual paralarvae, to examine individual variability and assess if paralarvae across treatments
411 retained consistent overall behavior patterns while in the 3D arena.

412 Since squid paralarvae swim in a characteristic cycle of vertical jetting and sinking, average
413 vertical velocity canceled out to zero. Therefore, vertical velocity was subdivided into average
414 positive vertical velocity, representative of upward jets, and negative vertical velocity,
415 representative of sinking and uncommon, but possible, downward jets. Average jet velocity was
416 calculated by measuring the magnitude of the peaks, above a threshold of 0.5 cm $s^{-1}$ (based on
417 visual assessment of the data and on a reported range of jetting velocities in Bartol et al., 2009a),
418 of the 3D velocity data across the two-minute recording period for each paralarvae. Jetting rate
419 was likewise calculated by enumerating these velocity peaks for each paralarvae.

420 Turning angles for each paralarva's path were calculated between sequential motion vectors
421 in the *x*, *y* plane at a resolution of thirty frames of video, or approximately one second of motion.
422 Tortuosity, a metric of path convolution defined as the ratio of the length of an animal's path to
423 the distance between the start and end points of that path, was calculated for each paralarva on
424 path segments of thirty frames of video continuously along the entire path (Benoit-Bird & Gilly,
425 2012). The one-second resolution for these metrics was chosen to analyze individual paralarval
426 paths on a reasonable temporal scale and reduce small-scale motion noise.

427 While thresholds of video quality and organism visibility limited the total number of videos
428 useable in the 3D tracking analysis, many more videos were useable for simpler analyses. In
429 some cases the side video was trackable or could be visually assessed while the top was not, so a
430 random subset (n = 282, Table 1) of 3D videos taken was analyzed for time spent in depth bins,
431 as in the 2D experiment. A separate randomly selected subset of approximately ten of the two-

minute paralarva swimming videos taken was analyzed per treatment per trial (n = 167, Table 1) for general ethography. Sections of each video were coded as either active, defined as a paralarvae jetting or pulsing its mantle, or inactive, defined as sinking, non-motile, and non-pulsing. Two observers each independently coded the same subset of 10 individual paralarvae to establish consistency in the definitions and then separately coded different subsets of the full dataset. Ethographic observations of activity were compiled as percent time active (converted from number of frames using the video frame rate) for the entire two-minute recording period for each individual paralarva.

*Statistics*

Statistical analyses were run in MATLAB, Python (3.5.2), and Excel. Normality was tested for using the Shapiro-Wilk test ($\alpha = 0.05$) and by examining quantile plots of the data for each factor, both within each treatment and as a whole. Datasets that were normally distributed were tested for differences among $CO_2$ treatments with a single factor ANOVA, while nonparametric data were tested with Kruskal-Wallis (KW) tests. Any significant ($p < 0.05$) KW test was subsequently run through a Dunn's posthoc test to determine which groups were significantly different from each other. Linear trend lines of the medians for each factor across $CO_2$ treatments were plotted in order to examine goodness of fit to the trend. Variability was examined through calculation of the variance, comparable within a metric, and the coefficient of variation (CV), which is comparable across metrics. All normally distributed statistics are reported as means ± 1 standard deviation (SD) while nonparametric statistics are reported as medians and interquartile range (IQR).

This is a post-peer-review, pre-copyedit version of an article published in Hydrobiologia. The final authenticated version is available online at: http://dx.doi.org/10.1007/s10750-017-3342-9

## Results

*Water Quality*

No significant differences (Kruskal-Wallis, $p > 0.05$ for $pH_{total}$ and $pCO_2$ for all trials) in water quality were seen between experimental cups within a treatment, so values are compiled and reported by treatment (Table 1). Temperature and salinity were stable across the duration of a trial, but varied slightly between trials, most likely due to local environmental variability. $pCO_2$ equilibrations were harder to control at higher concentrations, likely due to variability in the alkalinity and flow rate of ESL water (potentially due the expanded system, longer time frame, and increased demand in 2014 & 2015), as input gas concentrations and pressure were maintained throughout experiments and $pH_{total}$ remained consistent within trials (Table 1). Results are grouped and reported by input gas concentration for concision, but it should be noted that the 2200 ppm group encompasses a range from 1750 - 2400 ppm in calculated $pCO_2$ values.

*Experiment 1: 2D Depth*

Squid paralarvae showed a slight, but significant (KW, $p < 0.001$) difference in proportion of time spent in the top depth bin between $CO_2$ treatment groups in 2013 (Fig. 2A), but no significant response in 2014 (KW, $p = 0.078$)(Fig. 2B). In the compiled dataset, within the top depth bin, the 400 and 1300 ppm $CO_2$ treatment groups were found to be different from the 1900 and 2200 ppm treatment groups, with less time spent at surface in the higher $CO_2$ treatments (Table 2). Similarly, tests for proportion time spent in the middle and bottom depth bins also showed differences between treatment groups (KW, $p_{mid} = 0.001$, $p_{bottom} = 0.002$), wherein the 1300 ppm treatment group was distinct from the 1900 and 2200 ppm treatment groups, with more time spent in the middle and bottom depth bins in the higher $CO_2$ treatments

This is a post-peer-review, pre-copyedit version of an article published in Hydrobiologia. The final authenticated version is available online at: http://dx.doi.org/10.1007/s10750-017-3342-9

(Table 2). This reflects the extremely low variance in the 1300 ppm treatment group compared to all other treatments in all depth bins ($\sigma^2 \leq 0.001$, Table 3). Variance did not significantly increase with $CO_2$ level in the top or bottom depth bin, but showed an increasing trend with increasing $CO_2$ level in the middle depth bin ($R^2 = 0.609$, Table 3). Despite notable individual variability across treatments and interannual variability in response, the experiment indicated that squid paralarvae spent less time at the surface in $CO_2$ treatments of 1900 and 2200 ppm overall (Fig. 2C).

*Experiment 2: 3D Metrics*

In the 3D system, paralarvae showed no difference in the proportion of time spent in any depth bin across $CO_2$ treatments (KW, $p_{top} = 0.1094$, $p_{mid} = 0.0568$, $p_{bottom} = 0.0694$, Table 4) in all trials of both 2014 and 2015, nor were there any notable trends in the variance for this metric (Table 5). The proportion of time spent in the top depth bin showed a weak, non-significant decrease with increasing $pCO_2$ ($R^2 = 0.6455$) and proportions of time spent in the mid and bottom depth bins showed corresponding, non-significant increasing trends with increasing acidification (Table 4).

Of the 3D metrics measured for the paralarvae, total distance (KW, $p = 0.0342$), average velocity (KW, $p = 0.0354$), average positive vertical velocity (KW, $p = 0.0126$), and average negative vertical velocity (KW, $p = 0.0028$) showed significant effects of $CO_2$ treatment (Table 4). Dunn's posthoc test revealed the difference to be between the 400 and 1000 ppm groups for all of these metrics (Table 6). Average velocity was slightly higher in the 400 ppm treatment level, 9.4 mm $s^{-1}$ (8.2 - 11.7), compared to the other $CO_2$ treatments: 8.0 mm $s^{-1}$ (7.1 - 9.3), 8.3 mm $s^{-1}$ (7.6 - 9.9), and 8.2 mm $s^{-1}$ (7.0 - 9.7) for 1000, 1600, and 2200 ppm, respectively (Table

This is a post-peer-review, pre-copyedit version of an article published in Hydrobiologia. The final authenticated version is available online at: http://dx.doi.org/10.1007/s10750-017-3342-9

4). A linear fit ($R^2 = 0.4591$) of the median average velocities across treatments demonstrates this potential decreasing trend with increasing $pCO_2$. The step-wise nature of this trend is reflected in the average positive and negative vertical velocity values (Table 4), while the horizontal component of the velocity showed a significant fit to a linear decreasing trend ($R^2 = 0.9798$, $p = 0.0101$) rather than any significant differences between treatments (KW, $p = 0.1945$). Percent time active, as assessed in the ethological work, also followed a significant decreasing linear trend ($R^2 = 0.9798$, $p = 0.0077$), without significant differences between groups (KW, $p = 0.242$).

Analyzed individuals exhibited the expected, stereotypical motion of hatchling paralarvae, swimming with repeated, and dominantly vertical, jetting motions (Fig. 3). Average jet velocity was highest in the 400 ppm treatment, 17.6 mm $s^{-1}$ (14.2 - 19.6), and notably, but not significantly (KW, $p = 0.1192$) lower, in the 1000, 14.9 mm $s^{-1}$ (13.1 - 16.5), 1600, 14.7 mm $s^{-1}$ (13.0 - 16.9), and 2200 ppm, 15.1 mm $s^{-1}$ (12.5 - 17.9) treatments. Peak velocity was highest in the 400 ppm treatment, 139.6 mm $s^{-1}$ (99.9 - 206.9), and the 1000 ppm treatment, 138.2 mm $s^{-1}$ (78.8 - 228.7), notably lower in the 1600 ppm, 108.1 mm $s^{-1}$ (86.4- 163.3), and 2200 ppm treatments, 123.9 mm $s^{-1}$ (82.1 - 187.5), showing a weak decreasing linear trend ($R^2 = 0.4578$), but no statistical significance (KW, $p = 0.4378$). Vertical and horizontal peak velocities also show this pattern of more step-wise and weakly linear, non-significant decrease from 400 ppm (Table 4). Jetting rate, on the other hand, showed similar values between 400 ppm, 2.73 Jets $s^{-1}$ (2.51 - 3.02), 1000 ppm, 2.70 Jets $s^{-1}$ (2.51 - 2.89), and 1600 ppm, 2.72 Jets $s^{-1}$ (2.47 - 2.85), and only decreased slightly at 2200 ppm, 2.63 Jets $s^{-1}$ (2.38 - 2.81) (KW, $p = 0.3436$).

Three-dimensional polygons of volume transited, tortuosity paths, and turning angle distributions were also determined (Fig. 4). Volume traveled by the paralarvae during the

swimming recording was notably, but not significantly (KW, $p = 0.7416$) lower in the 2200 ppm treatment, 46,406 $mm^3$ (22,078 - 118,883), compared to the other treatments, 53,786 $mm^3$ (20,550 - 95,664), 65,076 $mm^3$ (33,647 - 125,970), and 53,315 $mm^3$ (30,734 - 103,950) for 400, 1000, and 1600 ppm respectively, and demonstrated a weakly decreasing linear trend ($R^2 = 0.4334$). Variance was high for volume transited across treatments ($\sigma^2$ range = $2.86 \times 10^9$ - $7.71 \times 10^9$, overall CV = 0.918) and appeared to increase with increasing $CO_2$ ($R^2 = 0.8710$, Table 5).

Average turning angle was highest in the 400 ppm treatment group, 56.53º (48.84º - 64.54º), whereas values were similar amongst the other treatments: 53.49º (48.45º - 62.04º), 52.05º (45.92º - 60.00º), and 52.30º (43.64º - 63.71º) for 1000, 1600, and 2200 ppm, respectively, resulting from a slightly higher occurrence of reversals in the 400 ppm group. Similar to other metrics, average turning angle was not statistically significant (KW, $p = 0.4334$), but still showed a slightly decreasing linear trend ($R^2 = 0.7863$). No apparent impacts of acidification on paralarval control of orientation were observed. Distributions of the turning angles from the entire paralarval path did not vary between treatments, except in the 120º - 130º bin where turns were rare (Average frequency of turns, 120 - 130º, all treatments $< 0.025$; $KW_{120\text{-}130}$, $p = 0.013$; KW, $p > 0.05$ for all other turning angle bins). All experimental paralarvae demonstrated primarily forward and reverse motions, due to the dominance of jetting, and a slightly higher frequency of shallow (10 - 40º) forward turns along their swimming paths.

Average tortuosity did not vary notably between $CO_2$ treatments (KW, $p = 0.6730$). It was highest in the 2200 ppm treatment, 3.63 (3.07 - 5.19), and lowest in the 1600 ppm treatment, 3.39 (2.92 - 4.51), showing a weakly increasing trend with increasing $CO_2$ ($R^2 = 0.4065$, Table 4).

546 Variance was higher in the 400 and 2200 ppm treatments than in the other $CO_2$
547 treatments for several metrics (total distance, average velocity, turning angle) (Table 5). Overall
548 variability, as demonstrated by the CV for each metric, was highest in peak velocities, average
549 vertical velocity components, volume transited, and average tortuosity (Table 5). Except for
550 volume transited, as previously noted, and average jet velocity, which had an increasing trend in
551 both variance and CV with increasing $CO_2$ ($\sigma^2$ $R^2 = 0.6506$, CV $R^2 = 0.8647$) variability did not
552 fit an increasing or decreasing trend across $CO_2$ treatments for the 3D metrics (Table 5). Patterns
553 of variance seen in the 3D metrics do not appear to align with variation in the total number of
554 individuals recorded for each CO2 treatment (Table 1). Although individual paralarvae were
555 quite variable over the course of their swimming path, medians and overall trends of the total
556 dataset were consistent across the entire recorded swimming period (KW, $p > 0.05$ across 10-
557 second time bins within $CO_2$ treatments for all 3D metrics) (Fig. 5).
558
559 **Discussion**
560 Paralarvae recorded in the 2D behavior arena demonstrated a decrease in time spent in
561 the top, near-surface depth bin at the highest $CO_2$ concentrations tested. Squid paralarvae are
562 negatively buoyant and "hop" with pulsed jetting to maintain their position in between sinks, the
563 rate of which could decrease with decreased available energy (Seibel et al., 2000). Squid jetting
564 comes at a high energetic cost, which has been proposed as a driver of their "live fast, die young"
565 lifestyle and highlighted as a limitation in their ability to compete directly with fish (O'Dor &
566 Webber, 1986). Propulsive efficiency, of just the jetting contraction phase, has been shown to be
567 quite high in *D. pealeii* paralarvae, greater than 80%, decreasing with growth to the juvenile &
568 adult phases (Bartol et al., 2008, 2009a). Modeled hydrodynamic efficiency for squid,

This is a post-peer-review, pre-copyedit version of an article published in Hydrobiologia. The final authenticated version is available online at: http://dx.doi.org/10.1007/s10750-017-3342-9

considering the whole jetting cycle, however, demonstrated that efficiency increases with growth from hatching to a peak efficiency of about 40% at 10 mm DML, decreasing slightly thereafter (Staaf et al., 2014). The decrease in time spent near the surface seen in high $CO_2$-exposed paralarvae in the 2D analysis may have been caused by a reallocation of available energy by these paralarvae towards stress response resulting in decreased swimming activity, a reduction in jetting efficiency due to slightly smaller mantle size (seen in Kaplan et al., 2013), or a combination thereof, resulting in increased time spent sinking. Limitations in the analytical power of the 2D system prevented further disentanglement of these factors.

The significant reductions in average 3D velocity and average positive vertical velocity, as well as the significant decreasing trend in paralarval activity from the 3D system, support the idea that acidification impacts the energetics of the paralarvae, even if effects are slight. Other observed metrics of 3D swimming activity did not demonstrate significant shifts across $CO_2$ levels, but exhibited decreasing patterns with increasing $CO_2$ exposure, further suggesting a subtle impact of acidification on the energetics and dynamics of swimming. Hypercapnia has been shown to depress energy expenditure rates in embryonic and pre-hatchling cuttlefish, *Sepia officinalis* (Rosa et al., 2013). Adults and juveniles of this species appear capable of withstanding chronic acidification through a system of branchial acid-base transporters, but embryos were seen to a downregulate ion regulatory and metabolic genes under increased acidification (Hu et al., 2011). Ion pump activities were seen to be even lower in the embryos and paralarvae of a Loliginid squid, *Loligo vulgaris*, than in *S. officinalis*, suggesting a greater pH sensitivity in this taxa (Hu et al., 2010). However, embryos of another squid, *Sepioteuthis lessoniana*, upregulated genes of a proton secretion pathway under severe chronic acidification ($pH_{nbs}$ = 7.31) demonstrating the potential for a powerful homeostatic response (Hu et al., 2013). Given that

This is a post-peer-review, pre-copyedit version of an article published in Hydrobiologia. The final authenticated version is available online at: http://dx.doi.org/10.1007/s10750-017-3342-9

592 cephalopod eggs naturally become acidified due to embryonic respiration over the course of
593 development, it is possible that, while variable, a general pH resilience is a conserved feature of
594 the class, which may serve to explain the weakness in OA responses seen here (Gutowska &
595 Melzner, 2009; Long et al., 2016).

596 The OA effects on vertical swimming in 2013 and decreasing trends in 3D swimming
597 behaviors in 2014 demonstrated a remarkable resilience, requiring intense, chronic exposures (>
598 1900 ppm) to acidification that *D. pealeii* should at most experience acutely in estuarine
599 environments (Jacobson, 2005; Baumann et al., 2014). These levels of acidification are predicted
600 in models only under a high emissions scenario after several hundred years (Caldeira & Wickett,
601 2003). Early physiological work exposing adult *D. pealeii* to hypercapnia noted the remarkable
602 $CO_2$ tolerance of this species, suggesting that even with the Bohr effect, decreased pH reducing
603 oxygen carrying capacity of their hemocyanin, they would not be significantly stressed unless
604 exposed to concurrent hypoxia (Redfield & Goodkind, 1929). Embryos of the California market
605 squid, *Doryteuthis opalescens*, which naturally experience sporadic pH reduction (down to 7.65)
606 due to upwelling, showed development delay and smaller statoliths under a combined regime of
607 OA (pH 7.57) and hypoxia (80μM), while under only decreased pH (7.56) showed a reduced
608 yolk volume, but larger statoliths compared to hypoxia alone (Navarro et al., 2016). Given the
609 substantial acid-base balancing machinery of cephalopods, it is possible that if subtle effects of
610 acidification are seen, particularly in relation to energy and activity, it is due to a slightly reduced
611 oxygen availability owing to the pH sensitivity of their hemocyanin, but that they are otherwise
612 fairly resistant to acidification in a well oxygenated system (Hu et al., 2010; Seibel, 2013).

613 While the 2013 2D depth results showed a clear impact of high, chronic acidification on
614 paralarval swimming behavior (Fig. 2A), no significant effect of $pCO_2$ on paralarval swimming

depth was seen in the 2014 2D trial and all subsequent 3D trials (run in 2014 & 2015) (Fig. 2B, Table 4), indicating a possible interannual or cohort-based variance in the strength of embryonic and paralarval response to this stressor. Seasonal cohorts of *L. vulgaris* eggs were shown to respond differentially to warming and OA, with the summer clutches showing greater sensitivity (Rosa et al., 2014). Murray et al. have demonstrated intraspecies seasonal variability in OA stress response for the Atlantic silverside, *Menidia menidia*, dependent on parental exposure and offspring conditioning (2014). The annual *D. pealeii* breeding cycle in Vineyard Sound is known to have some weak seasonal structuring with the earliest mating (April-May) involving robust two-year olds, while the rest of the breeding season is dominated by the previous year-class, however our data does not correlate with any clear seasonal signal (Arnold et al., 1974). Squid populations have been noted to demonstrate interannual variability, potentially as a plastic response of the year-class to environmental influence (Pecl et al., 2004). It is possible that an organism as plastic and fast-lived as *D. pealeii* could exhibit differential responses to stressors dependent on the experiences of the year-class and on how those adults condition their resultant offspring (Summers, 1971).

Considerable variability in behavior and response was seen individually within the paralarvae, both overall (Fig. 5) and across $CO_2$ treatments (Table 3, Table 5). Seemingly high variance may be partly due to moderate sample sizes in some treatments (Table 1). However, the distributions of variance across $CO_2$ treatments, and the high coefficients of variation for many 3D metrics, indicate a more prominent effect of individual variability (Table 5). Complexity and plasticity are hallmarks of the cephalopods, and individual variability is a strong benefit for fast-lived, highly fecund, r-selected organisms such as squid, as it provides adaptive flexibility in the face of rapid environmental change (Herke & Foltz, 2002; Pecl et al., 2004). While variability

638 between cohorts of eggs is likely due to differences in parentage, variability within a clutch is an
639 effect either of differential fathership and/or maternal condition (Buresch et al., 2001, 2009;
640 Steer et al., 2004). Intracapsular variability within a maternal clutch has been noted in the
641 elemental composition of statoliths, DML, and yolk volume in late stage *D. opalescens* embryos
642 (Navarro et al., 2014, 2016). Given the complexity of squid parentage, differential parental
643 conditioning and any resultant epigenetic effects might also express as differential responses or
644 behaviors, particularly when dealing with a stressor, as is seen in other marine species (Buresch
645 et al., 2001; Miller et al., 2012; Putnam & Gates, 2015). Maternal variation in transmitted yolk
646 content could have impacts on both the paralarval energy budget and their specific gravity, both
647 of which could translate to swimming behaviors (Vidal et al., 2002a; Martins et al., 2010).
648 Embryo position in the egg capsule itself, and the resultant exposure to differential levels of
649 hypoxia and acidification over development, could also explain the dynamic variability in
650 individual swimming behaviors and activities seen in our experiment (Long et al., 2016).
651 It is likely that our power to see effects caused by OA was reduced by this intense
652 individual variability and the logistical challenge of acquiring a large enough sample size of
653 useable paralarvae videos. Differences in the 2D system were only seen between those treatment
654 groups with either a substantial sample size of useable videos (400, 1900, and 2200 ppm, Table
655 1) or a particularly low variance (1300 ppm, Table 3). The videos resulting from the cubic arena
656 provided substantially clearer imagery and allowed both for better observation and tracking of
657 the squid paralarvae (Fig. 3, Fig. 4). An advantage of the new methodology implemented here is
658 that it is easily set up and repeated. We were limited primarily by our organism's breeding
659 window, the low ratio, for our paralarvae, of useable videos to videos taken, and the time needed
660 for experimentation and processing (Table 1)(Vecchione, 1981; Hastie et al., 2009).

Three-dimensional positional data acquired through observer corrected automated tracking in Tracker and processing in the 3D model equations described above resulted in clear tracks for each individual, similar to those determined by other established methods (Cachat et al., 2011b). Individual tracked paths produced by the system provide a powerful basis for analyzing movement patterns in marine and aquatic organisms. Total distance traveled and average velocity of the paralarvae were significantly different between the 400 and 1000 ppm groups, but most of the 3D metrics examined demonstrated only weakly decreasing trends with increasing $CO_2$ (Table 4). Average velocities for *D. pealeii* paralarvae recorded from the 3D system, 8.3 mm $s^{-1}$ ± 2.5 (median ± SD), fall within, but on the low end, of the range previously reported for the species during mantle contraction, 6.6 – 30.5 mm $s^{-1}$ (Bartol et al., 2009a). Limitations in these metrics may arise from the general, undirected swimming of the organisms. All the animals studied swam at about the same rate and for the same general distance; however, the absence of flow, predators, prey, conspecifics, or other major sensory cues throughout these tests should be noted. It is possible that potential acidification effects in the 3D swimming system did not emerge, both because of the high multi-scale variability and because the paralarvae were not sufficiently challenged in their motion. Sensory-driven experiments taking advantage of the squid paralarvae's innate photopositivity as a target may better elucidate stress effects by coercing the organism into predictable, directed motion.

Both arenas used likely enacted some influence over the behavior of the paralarvae. Both systems only allowed for a still water experimentation regime and did not provide analysis of the natural impacts of turbulence and flow that other methods, particularly DPIV, are capable of (Fuchs et al., 2004; Wheeler et al., 2015). Stillwater also resulted in a flat surface layer, which was necessary for filming from above, but also allowed for the influence of surface tension,

This is a post-peer-review, pre-copyedit version of an article published in Hydrobiologia. The final authenticated version is available online at: http://dx.doi.org/10.1007/s10750-017-3342-9

684 which was found to entrain paralarvae in the meniscus of the 2D system, and has been shown in
685 other studies to influence the speed and survival of marine larvae (Hidu & Haskin, 1978;
686 Yamaoka et al., 2000). Paralarval *D. pealeii* do not live in a still water environment, but instead
687 navigate the dynamic surface ocean; although their precise behaviors are not well known
688 (Vecchione et al., 2001; Barón, 2003; Jacobson, 2005). Therefore, while the system was
689 effective at exploring fundamental, physiologically-driven differences in hatchling swimming
690 capability it does not directly reflect how paralarval swimming behaviors might shift in response
691 to OA in the natural system or throughout ontogeny.

692 This study set out to examine the potential impacts of developmental exposure to OA on
693 the swimming behavior of hatchling squid paralarvae. The study required and inspired the
694 development of a novel, simple, and feasible system for recording, tracking, and analyzing the
695 3D motion of a motile marine larvae. Early results demonstrated an impact of high $CO_2$
696 exposures on paralarval activity and vertical positioning. Measured in the 3D system, average
697 velocity and average positive vertical velocity showed significant decreases from ambient, 400
698 ppm, to 1000 ppm, while horizontal velocity showed a significantly decreasing trend further
699 indicating an impact of OA on hatchling energetics. However, most metrics only demonstrated
700 subtle, nonsignificant, decreasing trends with decreased pH, supporting the idea that acidification
701 may be a weak stressor in cephalopods. Notable individual variability, as well as potential
702 interannual and/or cohort scale variability, was also seen in the response to acidification,
703 indicating a substantial plasticity and general pH resilience for the population. Further study into
704 the physiological tolerances and behavioral responses of this taxon would require incorporating
705 higher $CO_2$ levels, beyond 2200 ppm, or the introduction of compounding stressors in a
706 multifactor design. Replication of this and related stress experiments across multiple years would

707 also be required in order to better describe the patterns and drivers of individual, intra-annual,
708 and interannual variabilities. The 3D model system has potential utility in a wide variety of
709 applications, including complex tracking of aquatic or marine larvae from other taxa, tracking of
710 multiple individuals within the same arena, predator-prey interactions, as well as sensory studies.
711 The range of organismal responses to anthropogenically induced global ocean change continues
712 to grow in diversity and complexity as more taxa and stressors are examined. Improvements in
713 the accessibility of methods to address this ever-expanding field of questions are necessary in
714 order to facilitate and support this substantial effort.

715 References

716 Arkhipkin, A. I., & V. A. Bizikov, 2000. Role of the statolith in functioning of the acceleration
717 receptor system in squids and sepioids. Journal of Zoology 250: 31–55.

718 Arnold, J. M., W. C. Summers, D. L. Gilbert, R. S. Manalis, N. W. Daw, & R. J. Lasek, 1974. A
719 guide to laboratory use of the squid Loligo pealei. .

720 Barón, P. J., 2003. The paralarvae of two South American sympatric squid: Loligo gahi and
721 Loligo sanpaulensis. Journal of Plankton Research 25: 1347–1358.

722 Bartol, I. K., P. S. Krueger, W. J. Stewart, & J. T. Thompson, 2009a. Pulsed jet dynamics of
723 squid hatchlings at intermediate Reynolds numbers. The Journal of Experimental Biology 212:
724 1506–1518.

725 Bartol, I. K., P. S. Krueger, W. J. Stewart, & J. T. Thompson, 2009b. Hydrodynamics of pulsed
726 jetting in juvenile and adult brief squid Lolliguncula brevis: evidence of multiple jet “modes”
727 and their implications for propulsive efficiency. The Journal of Experimental Biology 212:
728 1889–1903.

729 Bartol, I. K., P. S. Krueger, J. T. Thompson, & W. J. Stewart, 2008. Swimming dynamics and
730 propulsive efficiency of squids throughout ontogeny. Integrative and Comparative Biology 48:
731 720–733.

732 Baumann, H., R. B. Wallace, T. Tagliaferri, & C. J. Gobler, 2014. Large Natural pH, CO2 and
733 O2 Fluctuations in a Temperate Tidal Salt Marsh on Diel, Seasonal, and Interannual Time
734 Scales. Estuaries and Coasts .

735 Beck, M. W., K. L. Heck, K. W. Able, D. L. Childers, D. B. Eggleston, B. M. Gillanders, B.
736 Halpern, C. G. Hays, K. Hoshino, T. J. Minello, R. J. Orth, P. F. Sheridan, & M. P. Weinstein,
737 2001. The Identification, Conservation, and Management of Estuarine and Marine Nurseries for
738 Fish and Invertebrates. BioScience 51: 633.

739 Benoit-Bird, K. J., & W. F. Gilly, 2012. Coordinated nocturnal behavior of foraging jumbo squid
740 Dosidicus gigas. Marine Ecology Progress Series 455: 211–228.

This is a post-peer-review, pre-copyedit version of an article published in Hydrobiologia. The final authenticated version is available online at: http://dx.doi.org/10.1007/s10750-017-3342-9

741 Boisclair, D., 1992. An Evaluation of the Stereocinematographic Method to Estimate Fish
742 Swimming Speed. Canadian Journal of Fisheries and Aquatic Sciences 49: 523–531.

743 Budick, S. A., & D. M. O'Malley, 2000. Locomotor repertoire of the larval zebrafish:
744 swimming, turning and prey capture. The Journal of Experimental Biology 203: 2565–2579.

745 Buresch, K. C., M. R. Maxwell, M. R. Cox, & R. T. Hanlon, 2009. Temporal dynamics of
746 mating and paternity in the squid Loligo pealeii. Marine Ecology Progress Series 387: 197–203.

747 Buresch, K. M., R. T. Hanlon, M. R. Maxwell, & S. Ring, 2001. Microsatellite DNA markers
748 indicate a high frequency of multiple paternity within individual field-collected egg capsules of
749 the squid Loligo pealeii. Marine Ecology Progress Series 210: 161–165.

750 Byrne, M., 2011. Impact of ocean warming and ocean acidification on marine invertebrate life
751 history stages : Vulnerabilities and potential for persistence in a changing ocean. Oceanogr. Mar.
752 Biol. Annu. Rev. 49: 1–42.

753 Cachat, J. M., P. R. Canavello, S. I. Elkhayat, B. K. Bartels, P. C. Hart, M. F. Elegante, C.
754 Esther, A. L. Laffoon, W. A. M. Haymore, D. H. Tien, A. K. Tien, S. Mohnot, & A. V Kalueff,
755 2011a. Chapter 16: Deconstructing Adult Zebrafish Behavior with Swim Trace Visualizations In
756 Kalueff, A. V., & J. M. Cachat (eds), Zebrafish Neurobehavioral Protocols. : 191–201.

757 Cachat, J., A. Stewart, E. Utterback, P. Hart, S. Gaikwad, K. Wong, E. Kyzar, N. Wu, & A. V.
758 Kalueff, 2011b. Three-dimensional neurophenotyping of adult zebrafish behavior. PLoS ONE 6.

759 Caldeira, K., & M. E. Wickett, 2003. Oceanography: anthropogenic carbon and ocean pH.
760 Nature 425: 365.

761 Coughlin, D. J., J. R. Strickler, & B. Sanderson, 1992. Swimming and Search Behavior in
762 Clownfish, Amphiprion-Perideraion, Larvae. Animal Behaviour 44: 427–440.

763 Doney, S. C., V. J. Fabry, R. A. Feely, & J. A. Kleypas, 2009. Ocean acidification: the other
764 CO2 problem. Annual Review of Marine Science 1: 169–192.

765 Fuchs, H. L., L. S. Mullineaux, & A. R. Solow, 2004. Sinking behavior of gastropod larvae
766 (Ilyanassa obsoleta) in turbulence. Limnology and Oceanography 49: 1937–1948.

767 Gledhill, D. ., M. . White, J. Salisbury, H. Thomas, I. Misna, M. Liebman, B. Mook, J. Grear, A.
768 C. Candelmo, R. C. Chambers, C. J. Gobler, C. W. Hunt, A. L. King, N. N. Price, S. R.
769 Signorini, E. Stancioff, C. Stymiest, R. A. Wahle, J. D. Waller, N. D. Rebuck, & Z. A. Wang,
770 2015. Ocean and coastal acidification off New England and Nova Scotia. Oceanography 28:
771 182–197.

772 Guppy, M., & P. Withers, 1999. Metabolic depression in animals: physiological perspectives and
773 biochemical generalizations. Biological reviews of the Cambridge Philosophical Society 74: 1–
774 40.

775 Gutowska, M. A., & F. Melzner, 2009. Abiotic conditions in cephalopod (Sepia officinalis) eggs:
776 Embryonic development at low pH and high pCO2. Marine Biology 156: 515–519.

777 Gutowska, M. A., F. Melzner, M. Langenbuch, C. Bock, G. Claireaux, & H. O. Pörtner, 2010.
778 Acid–base regulatory ability of the cephalopod (Sepia officinalis) in response to environmental
779 hypercapnia. Journal of Comparative Physiology B 180: 323–335.

780 Hanlon, R., J. Bidwell, & R. Tait, 1989. Strontium is required for statolith development and thus
781 normal swimming behaviour of hatchling cephalopods. Journal of Experimental Biology 141:

187–195.

Hanlon, R. T., R. F. Hixon, & W. H. Hulet, 1983. Survival, growth, and behavior of the loliginid squids Logi plei, Loligo pealei, and Lolliguncula brevis (Mollusca: Cephalopoda) in closed sea water systems. Biology Bulletin 637–685.

Hastie, L. C., G. J. Pierce, J. Wang, I. Bruno, & A. Moreno, 2009. Cephalopods in the North-Eastern Atlantic: Species, Biogeography, Ecology, Exploitation and Conservation. Oceanography and Marine Biology: An Annual Review 47: 111–190.

Haury, L., & D. Weihs, 1976. Energetically efficient swimming behavior of negatively buoyant zooplankton. Limnology and Oceanography 21: 797–803.

Herke, S. W., & D. W. Foltz, 2002. Phylogeography of two squid (Loligo pealei and L. plei) in the Gulf of Mexico and northwestern Atlantic Ocean. Marine Biology 140: 103–115.

Hidu, H., & H. H. Haskin, 1978. Swimming speeds of oyster larvae Crassostrea virginica in different salinities and temperatures. Estuaries 1: 252–255.

Honisch, B., A. Ridgwell, D. N. Schmidt, E. Thomas, S. J. Gibbs, A. Sluijs, R. Zeebe, L. Kump, R. C. Martindale, S. E. Greene, W. Kiessling, J. Ries, J. C. Zachos, D. L. Royer, S. Barker, T. M. Marchitto, R. Moyer, C. Pelejero, P. Ziveri, G. L. Foster, & B. Williams, 2012. The Geological Record of Ocean Acidification. Science 335: 1058–1063.

Hu, M. Y., J.-R. Lee, L.-Y. Lin, T.-H. Shih, M. Stumpp, M.-F. Lee, P.-P. Hwang, & Y.-C. Tseng, 2013. Development in a naturally acidified environment: Na+/H+-exchanger 3-based proton secretion leads to CO2 tolerance in cephalopod embryos. Frontiers in zoology 10: 51.

Hu, M. Y., E. Sucre, M. Charmantier-Daures, G. Charmantier, M. Lucassen, N. Himmerkus, & F. Melzner, 2010. Localization of ion-regulatory epithelia in embryos and hatchlings of two cephalopods. Cell and Tissue Research 339: 571–583.

Hu, M. Y., Y.-C. Tseng, M. Stumpp, M. A. Gutowska, R. Kiko, M. Lucassen, & F. Melzner, 2011. Elevated seawater $PCO_2$ differentially affects branchial acid-base transporters over the course of development in the cephalopod Sepia officinalis. American journal of physiology. Regulatory, integrative and comparative physiology 300: R1100–R1114.

Hunsicker, M. E., & T. E. Essington, 2008. Evaluating the potential for trophodynamic control of fish by the longfin inshore squid (Loligo pealeii) in the Northwest Atlantic Ocean. Canadian Journal of Fisheries and Aquatic Sciences 65: 2524–2535.

Jacobson, L. D., 2005. Longfin Inshore Squid, *Loligo pealeii*, Life History and Habitat Characteristics. NOAA Technical Memorandum NMFS-NE.

Kaplan, M. B., T. A. Mooney, D. C. McCorkle, & A. L. Cohen, 2013. Adverse Effects of Ocean Acidification on Early Development of Squid (Doryteuthis pealeii). PLOS ONE 8.

Klimley, A. P., & S. T. Brown, 1983. Stereophotography for the field biologist: measurement of lengths and three-dimensional positions of free-swimming sharks. Marine Biology 74: 175–185.

Long, M. H., T. A. Mooney, & C. Zakroff, 2016. Extreme low oxygen and decreased pH conditions naturally occur within developing squid egg capsules. Marine Ecology Progress Series 550: 111–119.

Macy III, W. K., 1982. Feeding Patterns of the Long-Finned Squid, Loligo pealei, in New England Waters. Biological Bulletin 162: 28–38.

This is a post-peer-review, pre-copyedit version of an article published in Hydrobiologia. The final authenticated version is available online at: http://dx.doi.org/10.1007/s10750-017-3342-9

823 Macy III, W. K., & J. K. T. Brodziak, 2001. Seasonal maturity and size at age of Loligo pealeii
824 in waters of southern New England. ICES Journal of Marine Science 58: 852–864.

825 Martins, R. S., M. J. Roberts, N. Chang, P. Verley, C. L. Moloney, & E. a G. Vidal, 2010. Effect
826 of yolk utilization on the specific gravity of chokka squid (Loligo reynaudii) paralarvae:
827 Implications for dispersal on the Agulhas Bank, South Africa. ICES Journal of Marine Science
828 67: 1323–1335.

829 Maxwell, M. R., & R. T. Hanlon, 2000. Female reproductive output in the squid Loligo pealeii:
830 Multiple egg clutches and implications for a spawning strategy. Marine Ecology Progress Series
831 199: 159–170.

832 McCorkle, D. C., C. Weidman, & A. L. Cohen, 2012. Time series of pCO2, pH, and aragonite
833 saturation state in Waquoit Bay National Estuarine Research Reserve: "estaurine acidification"
834 and shellfish. Ocean Sciences Meeting. Salt Lake City, UT.

835 McMahon, J. J., & W. C. Summers, 1971. Temperature effects on the developmental rate of
836 squid (Loligo pealei) embryos. The Biological Bulletin 141: 561–567.

837 Messenger, J. B., 1970. Optomotor responses and nystagmus in intact, blinded and statocystless
838 cuttlefish (Sepia officinalis L.). The Journal of experimental biology 53: 789–796.

839 Miller, G. M., S.-A. Watson, J. M. Donelson, M. I. McCormick, & P. L. Munday, 2012. Parental
840 environment mediates impacts of increased carbon dioxide on a coral reef fish. Nature Climate
841 Change Nature Publishing Group 2: 858–861.

842 Murray, C. S., A. Malvezzi, C. J. Gobler, & H. Baumann, 2014. Offspring sensitivity to ocean
843 acidification changes seasonally in a coastal marine fish. Marine Ecology Progress Series 504:
844 1–11.

845 Navarro, M. O., E. E. Bockmon, C. A. Frieder, J. P. Gonzalez, & L. A. Levin, 2014.
846 Environmental pH, O2 and Capsular Effects on the Geochemical Composition of Statoliths of
847 Embryonic Squid Doryteuthis opalescens. Water 2233–2254.

848 Navarro, M. O., G. T. Kwan, O. Batalov, C. Y. Choi, N. T. Pierce, & L. A. Levin, 2016.
849 Development of Embryonic Market Squid, Doryteuthis opalescens, under Chronic Exposure to
850 Low Environmental pH and [O2]. Plos One 11.

851 O'Dor, R. K., & D. M. Webber, 1986. The constraints on cephalopods: why squid aren't fish.
852 Canadian Journal of Zoology 64: 1591–1605.

853 Pecl, G. T., N. A. Moltschaniwskyj, S. R. Tracey, & A. R. Jordan, 2004. Inter-annual plasticity
854 of squid life history and population structure: Ecological and management implications.
855 Oecologia 139: 515–524.

856 Putnam, H. M., & R. D. Gates, 2015. Preconditioning in the reef-building coral Pocillopora
857 damicornis and the potential for trans-generational acclimatization in coral larvae under future
858 climate change conditions. Journal of Experimental Biology 218: 2365–2372.

859 Redfield, A. C., & R. Goodkind, 1929. The Significance of the Bohr Effect in the Respiration
860 and Asphyxiation of the squid, Loligo pealei. Journal of Experimental Biology 6: 340–349.

861 Robin, J. P., M. Roberts, L. Zeidberg, I. Bloor, A. Rodriguez, F. Briceño, N. Downey, M.
862 Mascaró, M. Navarro, A. Guerra, J. Hofmeister, D. D. Barcellos, S. A. P. Lourenço, C. F. E.
863 Roper, N. A. Moltschaniwskyj, C. P. Green, & J. Mather, 2014. Transitions during cephalopod

life history: The role of habitat, environment, functional morphology and behaviour. Advances in Marine Biology.

Rosa, R., K. Trübenbach, M. S. Pimentel, J. Boavida-Portugal, F. Faleiro, M. Baptista, G. Dionísio, R. Calado, H. O. Pörtner, & T. Repolho, 2014. Differential impacts of ocean acidification and warming on winter and summer progeny of a coastal squid (Loligo vulgaris). The Journal of Experimental Biology 217: 518–525.

Rosa, R., K. Trübenbach, T. Repolho, M. Pimentel, F. Faleiro, J. Boavida-Portugal, M. Baptista, V. M. Lopes, G. Dionísio, M. C. Leal, R. Calado, & H. O. Pörtner, 2013. Lower hypoxia thresholds of cuttlefish early life stages living in a warm acidified ocean. Proceedings of the Royal Society B: Biological Sciences 280: 20131695.

Seibel, B. A., 2013. The jumbo squid, Dosidicus gigas (Ommastrephidae), living in oxygen minimum zones II: Blood-oxygen binding. Deep-Sea Research Part II: Topical Studies in Oceanography Elsevier 95: 139–144.

Seibel, B. A., F. G. Hochberg, & D. B. Carlini, 2000. Life history of Gonatus onyx (Cephalopoda: Teuthoidea): deep-sea spawning and post-spawning egg care. Marine Biology 137: 519–526.

Shashar, N., & R. T. Hanlon, 2013. Spawning behavior dynamics at communal egg beds in the squid Doryteuthis (Loligo) pealeii. Journal of Experimental Marine Biology and Ecology 447: 65–74.

Sokolova, I. M., 2013. Energy-limited tolerance to stress as a conceptual framework to integrate the effects of multiple stressors. Integrative and Comparative Biology 53: 597–608.

Sokolova, I. M., M. Frederich, R. Bagwe, G. Lannig, & A. A. Sukhotin, 2012. Energy homeostasis as an integrative tool for assessing limits of environmental stress tolerance in aquatic invertebrates. Marine Environmental Research 79: 1–15.

Staaf, D. J., W. F. Gilly, & M. W. Denny, 2014. Aperture effects in squid jet propulsion. The Journal of Experimental Biology 217: 1588–1600.

Stamhuis, E., & J. Videler, 1995. Quantitative flow analysis around aquatic animals using laser sheet particle image velocimetry. The Journal of Experimental Biology 198: 283–294.

Steer, M. A., N. A. Moltschaniwskyj, D. S. Nichols, & M. Miller, 2004. The role of temperature and maternal ration in embryo survival: Using the dumpling squid Euprymna tasmanica as a model. Journal of Experimental Marine Biology and Ecology 307: 73–89.

Summers, W. C., 1971. Age and growth of Loligo pealei, a population study of the common Atlantic coast squid. Biological Bulletin 141: 189–201.

Summers, W. C., J. J. McMahon, & G. N. P. A. Ruppert, 1974. Studies on the Maintenance of Adult Squid (Loligo Peali). II. Empirical Extensions. Biological Bulletin 146: 291–301.

Vecchione, M., 1981. Aspects of the early life history of Loligo pealeii (Cephalopoda; Myopsida). Journal of Shellfish Research 1: 171–180.

Vecchione, M., C. F. E. Roper, M. J. Sweeney, & C. C. Lu, 2001. Distribution , Relative Abundance and Developmental Morphology of Paralarval Cephalopods in the Western North Atlantic Ocean Paralarval Cephalopods in the. NOAA Technical Reports NMFS 152:.

Vidal, E. A. G., F. P. DiMarco, J. H. Wormuth, & P. G. Lee, 2002a. Influence of Temperature

905 and Food Availability on Survival , Growth and Yolk Utilization in Hatchling Squid. Bulletin of
906 Marine Science 71: 915–931.

907 Vidal, E. A. G., F. P. DiMarco, J. H. Wormuth, & P. G. Lee, 2002b. Optimizing rearing
908 conditions of hatchling loliginid squid. Marine Biology 140: 117–127.

909 Villanueva, R., C. Nozais, & S. V. Boletzky, 1997. Swimming behaviour and food searching in
910 planktonic Octopus vulgaris Cuvier from hatching to settlement. Journal of Experimental Marine
911 Biology and Ecology 208: 169–184.

912 Vogel, S., 1981. Life in Moving Fluids: The Physical Biology of Flow. Princeton University
913 Press, Princeton, New Jersey.

914 Wang, Z. A., R. Wanninkhof, W.-J. Cai, R. H. Byrne, X. Hu, T.-H. Peng, & W.-J. Huang, 2013.
915 The marine inorganic carbon system along the Gulf of Mexico and Atlantic coasts of the United
916 States : Insights from a transregional coastal carbon study. Limnology and Oceanography 58:
917 325–342.

918 Wassersug, R., & K. von Seckendorf Hoff, 1985. The kinematics of swimming in anuran larvae.
919 Journal of experimental biology 119: 1–30.

920 Wheeler, J. D., K. R. Helfrich, E. J. Anderson, B. McGann, P. Staats, A. E. Wargula, K. Wilt, &
921 L. S. Mullineaux, 2013. Upward swimming of competent oyster larvae Crassostrea virginica
922 persists in highly turbulent flow as detected by PIV flow subtraction. Marine Ecology Progress
923 Series 488: 171–185.

924 Wheeler, J. D., K. R. Helfrich, E. J. Anderson, & L. S. Mullineaux, 2015. Isolating the
925 hydrodynamic triggers of the dive response in eastern oyster larvae. Limnology and
926 Oceanography.

927 Yamaoka, K., T. Nanbu, M. Miyagawa, T. Isshiki, & a. Kusaka, 2000. Water surface tension-
928 related deaths in prelarval red-spotted grouper. Aquaculture 189: 165–176.

929 York, C. A., & I. K. Bartol, 2016. Anti-predator behavior of squid throughout ontogeny. Journal
930 of Experimental Marine Biology and Ecology Elsevier B.V. 480: 26–35.

931 Zeidberg, L. D., G. Isaac, C. L. Widmer, H. Neumeister, & W. F. Gilly, 2011. Egg capsule hatch
932 rate and incubation duration of the California market squid, Doryteuthis (=Loligo) opalescens:
933 Insights from laboratory manipulations. Marine Ecology 32: 468–479.

934

935

936

937

938

939

940

941

942

943

This is a post-peer-review, pre-copyedit version of an article published in Hydrobiologia. The final authenticated version is available online at: http://dx.doi.org/10.1007/s10750-017-3342-9

944

945

946 Tables

**Table 1.** Description of behavioral experiments divided by arena type, year, and trial. Seawater chemistry of $CO_2$ treatments for experimental squid egg capsule rearing cups (n = 4 cups per treatment level, 3 with squid egg capsules and 1 control) for all 2013, 2014, & 2015 behavior trials are provided. Values are reported as means with standard deviation. The total number of videos taken for each treatment is listed. Of the videos taken, only subsets of useable videos, those in which paralarvae were behaving normally and were either visually assessable or trackable by software, were used in the subsequent analyses

| Arena | Year | Trial | Laying Date | Treatment $CO_2$ (ppm) | Temp (°C) | $pH_{Total}$ | Salinity | $A_T$ (mmol $kgSW^{-1}$) | $\Omega_{Arag}$ | $pCO_2$ (ppm) | Videos Taken | Useable/Analyzed Videos | | |
|---|---|---|---|---|---|---|---|---|---|---|---|---|---|---|
| | | | | | | | | | | | | Depth Bins | Ethology | 3D Tracks |
| 2D | 2013 | 1 | 03-Jul | Ambient (550) | 20.83 (0.19) | 7.88 (0.02) | 31.40 (0.06) | 2060.3 (12.5) | 1.87 (0.08) | 565.68 (43.90) | 20 | 7 | - | - |
| | | | | 1300 | 20.83 (0.19) | 7.54 (0.01) | 31.41 (0.03) | 2064.7 (6.6) | 0.93 (0.04) | 1350.51 (43.55) | 18 | 13 | - | - |
| | | | | 2200 | 20.83 (0.19) | 7.34 (0.01) | 31.39 (0.05) | 2064.9 (16.1) | 0.60 (0.04) | 2199.56 (173.47) | 20 | 11 | - | - |
| | | 2 | 11-Jul | 850 | 20.46 (0.03) | 7.66 (0.01) | 31.26 (0.13) | 2042.1 (30.3) | 1.17 (0.03) | 987.43 (20.30) | 45 | 36 | - | - |
| | | | | 1300 | 20.46 (0.03) | 7.54 (0.03) | 31.29 (0.07) | 2051.6 (10.2) | 0.90 (0.03) | 1351.67 (34.26) | 46 | 21 | - | - |
| | | | | 2200 | 20.46 (0.03) | 7.31 (0.01) | 31.25 (0.13) | 2047.1 (21.2) | 0.54 (0.02) | 2380.50 (70.62) | 45 | 30 | - | - |
| | | 4 | 07-Aug | 400 | 19.97 (0.49) | 7.93 (0.01) | 31.51 (0.01) | 2032.0 (20.0) | 1.95 (0.00) | 488.58 (10.50) | 69 | 44 | - | - |
| | | | | 1900 | 19.97 (0.49) | 7.37 (0.00) | 31.46 (0.02) | 2015.8 (5.7) | 0.59 (0.00) | 2003.79 (12.84) | 75 | 67 | - | - |
| | | | | 2200 | 19.97 (0.49) | 7.35 (0.01) | 31.45 (0.02) | 2028.1 (0.0) | 0.56 (0.01) | 2130.17 (40.31) | 97 | 84 | - | - |
| 3D | 2014 | 1 | 29-May | 400 | 20.32 (0.18) | 7.97 (0.02) | 32.21 (0.13) | 2188.2 (32.4) | 2.27 (0.11) | 471.27 (28.31) | 46 | 27 | - | - |
| | | | | 1500 | 20.32 (0.18) | 7.55 (0.01) | 32.17 (0.05) | 2176.4 (33.4) | 0.98 (0.04) | 1403.10 (22.78) | 47 | 15 | - | - |
| | | | | 1700 | 20.32 (0.18) | 7.48 (0.00) | 32.17 (0.04) | 2179.5 (20.7) | 0.85 (0.02) | 1635.81 (23.56) | 43 | 21 | - | - |
| | | | | 2200 | 20.32 (0.18) | 7.40 (0.02) | 32.12 (0.05) | 2176.6 (22.3) | 0.69 (0.03) | 2001.40 (103.08) | 62 | 18 | - | - |
| | | 2 | 02-Jul | 400 | 20.65 (0.20) | 7.99 (0.05) | 32.37 (0.33) | 2140.6 (18.3) | 2.39 (0.21) | 439.52 (58.83) | 74 | 17 | 10 | 0 |
| | | | | 1000 | 20.65 (0.20) | 7.68 (0.01) | 32.13 (0.23) | 2137.9 (17.9) | 1.28 (0.04) | 982.22 (27.04) | 45 | 13 | 11 | 4 |
| | | | | 1600 | 20.65 (0.20) | 7.49 (0.01) | 32.18 (0.19) | 2136.0 (18.2) | 0.86 (0.03) | 1565.44 (40.27) | 79 | 25 | 12 | 3 |
| | | | | 2200 | 20.65 (0.20) | 7.44 (0.07) | 32.13 (0.24) | 2134.5 (20.2) | 0.77 (0.12) | 1787.99 (282.04) | 40 | 9 | 11 | 4 |
| | 2014 | 3 | 18-Jul | 400 | 20.24(0.08) | 7.99 (0.02) | 31.84 (0.50) | 2097.8 (19.5) | 2.25 (0.08) | 439.87 (24.74) | 71 | 26 | 10 | 10 |
| | | | | 1000 | 20.24(0.08) | 7.70 (0.01) | 31.88 (0.34) | 2104.3 (19.6) | 1.27 (0.04) | 934.49 (34.46) | 80 | 19 | 12 | 11 |
| | | | | 1600 | 20.24(0.08) | 7.49 (0.01) | 31.99 (0.34) | 2112.3 (37.8) | 0.82 (0.02) | 1562.37 (45.50) | 77 | 17 | 10 | 10 |
| | | | | 2200 | 20.24(0.08) | 7.38 (0.03) | 31.93 (0.37) | 2104.9 (23.1) | 0.65 (0.03) | 2033.82 (136.79) | 74 | 25 | 10 | 13 |
| | | 4 | 05-Sep | 400 | 20.73 (0.23) | 8.00 (0.03) | 32.75 (0.09) | 2096.0 (19.4) | 2.39 (0.12) | 418.25 (31.45) | 78 | 18 | 10 | 10 |
| | | | | 1000 | 20.73 (0.23) | 7.72 (0.03) | 32.43 (0.16) | 2090.1 (17.3) | 1.38 (0.09) | 856.00 (53.73) | 91 | 18 | 11 | 11 |
| | | | | 1600 | 20.73 (0.23) | 7.56 (0.04) | 32.42 (0.27) | 2087.3 (13.9) | 0.98 (0.08) | 1290.21 (128.77) | 78 | 17 | 10 | 11 |
| | | | | 2200 | 20.73 (0.23) | 7.40 (0.03) | 32.43 (0.15) | 2090.1 (19.8) | 0.69 (0.05) | 1909.49 (148.80) | 69 | 17 | 10 | 12 |
| | 2015 | 1 | 22-May | 400 | 20.36 (0.44) | 7.98 (0.04) | 33.10 (0.16) | 2201.4 (18.7) | 2.44 (0.18) | 454.10 (51.43) | 68 | 17 | 10 | 17 |
| | | | | 1000 | 20.36 (0.44) | 7.75 (0.02) | 33.00 (0.10) | 2189.7 (17.7) | 1.53 (0.05) | 828.19 (34.32) | 42 | 16 | 10 | 12 |
| | | | | 1600 | 20.36 (0.44) | 7.58 (0.03) | 32.97 (0.07) | 2197.5 (19.8) | 1.05 (0.06) | 1313.09 (100.28) | 30 | 15 | 10 | 16 |
| | | | | 2200 | 20.36 (0.44) | 7.46 (0.03) | 32.99 (0.09) | 2202.6 (20.7) | 0.81 (0.05) | 1770.29 (97.62) | 55 | 13 | 10 | 13 |

This is a post-peer-review, pre-copyedit version of an article published in Hydrobiologia. The final authenticated version is available online at: http://dx.doi.org/10.1007/s10750-017-3342-9

| Experiment | 1 | 2 |
|---|---|---|

947
948

**Table 2** Significant Dunn's posthoc test statistics for differences between $CO_2$ treatments within all depth bins examined. Data compiled from all trials of Experiment 1, $Q_{crit} = 3.12$

| $CO_2$ Treatment (ppm) | 1900 Top | 2200 Top | 1900 Mid | 2200 Mid | 1900 Bottom | 1900 Bottom |
|---|---|---|---|---|---|---|
| 400 Top | 3.52 | 3.72 | - | - | - | - |
| 1300 Top | 3.97 | 4.06 | - | - | - | - |
| 1300 Middle | - | - | 3.21 | 3.36 | - | - |
| 1300 Bottom | - | - | - | - | 3.58 | 3.74 |

949
950

**Table 3** Variance of 2D depth bins per $CO_2$ level compiled over all trials of Experiment 1. $R^2$ are of fits of linear trend lines ($p > 0.05$ for all regressions)

| $\sigma^2$ | 400 ppm | 550 ppm | 850 ppm | 1300 ppm | 1500 ppm | 1700 ppm | 1900 ppm | 2200 ppm | $R^2$ |
|---|---|---|---|---|---|---|---|---|---|
| 2D Top | 0.105 | 0.143 | 0.036 | 0.001 | 0.178 | 0.047 | 0.156 | 0.156 | 0.054 |
| 2D Middle | 0.006 | 0.000 | 0.007 | 0.001 | 0.027 | 0.033 | 0.015 | 0.036 | 0.609 |
| 2D Bottom | 0.091 | 0.129 | 0.023 | 0.000 | 0.117 | 0.005 | 0.156 | 0.116 | 0.015 |

951
952

**Table 4** Values of the 3D swimming behavior metrics at each $CO_2$ treatment. Reported values are medians and IQR. Significant Kruskal-Wallis p values marked with * ($p < 0.05$). $R^2$ are of fits of linear trend lines. Significant regressions are marked with * ($p < 0.05$).

| 3D Metric | 400 ppm | 1000 ppm | 1600 ppm | 2200 ppm | KW p value | $R^2$ |
|---|---|---|---|---|---|---|
| 3D Top (% Frames) | 0.95 (0.64 - 1.00) | 0.88 (0.53 - 1.00) | 0.92 (0.72 - 1.00) | 0.81 (0.43 - 0.98) | 0.1094 | 0.6455 |
| 3D Mid (% Frames) | 0.01 (0.00 - 0.12) | 0.07 (0.00 - 0.21) | 0.05 (0.00 - 0.13) | 0.06 (0.00 - 0.17) | 0.0568 | 0.5030 |
| 3D Bottom (% Frames) | 0.00 (0.00 - 0.16) | 0.03 (0.00 - 0.17) | 0.00 (0.00 - 0.08) | 0.04 (0.00 - 0.30) | 0.0694 | 0.3775 |
| Ethology (% Active) | 95.8 (88.1 - 100) | 93.8 (86.5 - 100) | 91.7 (68.5 - 99.4) | 88.3 (69.2 - 100) | 0.242 | 0.9847* |
| Total Distance (mm) | 1128.7 (985.1 - 1403.9) | 961.8 (855.7 - 1116.3) | 997.9 (912.5 - 1187.9) | 985.4 (840.2 - 1165.6) | 0.0342* | 0.4590 |
| Average Velocity (mm $s^{-1}$) | 9.4 (8.2 - 11.7) | 8.0 (7.1 - 9.3) | 8.3 (7.6 - 9.9) | 8.2 (7.0 - 9.7) | 0.0354* | 0.4590 |
| Peak Velocity (mm $s^{-1}$) | 139.6 (99.9 - 206.9) | 138.2 (78.8- 228.7) | 108.1 (86.4 - 163.3) | 123.9 (82.1 - 187.5) | 0.4378 | 0.4578 |
| Average Jet Velocity (mm $s^{-1}$) | 17.6 (14.2 - 19.6) | 14.9 (13.1 - 16.5) | 14.7 (13.0 - 16.9) | 15.1 (12.5 - 17.9) | 0.1192 | 0.5168 |
| Jetting Rate (Jets $s^{-1}$) | 2.73 (2.51 - 3.02) | 2.70 (2.51 - 2.89) | 2.72 (2.47 - 2.85) | 2.63 (2.38 - 2.81) | 0.3436 | 0.6270 |
| Average Vertical Velocity (mm $s^{-1}$) | 0.0 (-0.1 - 0.1) | 0.0 (-0.1 - 0.3) | 0.1 (0.0 - 0.4) | 0.0 (-0.1 - 0.3) | 0.1935 | 0.0678 |
| Average Positive Vertical Velocity (mm $s^{-1}$) | 9.6 (7.9 - 10.6) | 8.7 (6.8 - 9.3) | 8.7 (7.1 - 9.6) | 8.7 (7.4 - 9.7) | 0.0126* | 0.5540 |
| Peak Vertical Velocity (mm $s^{-1}$) | 100.3 (75.0 - 150.6) | 83.8 (60.6 - 138.3) | 85.9 (62.4 - 127.0) | 83.2 (66.6 - 106.9) | 0.2584 | 0.6194 |

This is a post-peer-review, pre-copyedit version of an article published in Hydrobiologia. The final authenticated version is available online at: http://dx.doi.org/10.1007/s10750-017-3342-9

| | | | | | | |
|---|---|---|---|---|---|---|
| Average Negative Vertical Velocity (mm $s^{-1}$) | -5.7 (-6.2 - -4.9) | -4.6 (-5.3 - -3.9) | -4.9 (-5.9 - -4.3) | -5.0 (-5.7 - -4.5) | 0.0028* | 0.2847 |
| Minimum Vertical Velocity (mm $s^{-1}$) | -83.5 (-122.2 - -62.8) | -63.1 (-118.6 - -44.5) | -74.9 (-101.4 - -54.6) | -79.9 (-117.1 - -49.5) | 0.4982 | 0.0002 |
| Average Horizontal Velocity (mm $s^{-1}$) | 4.6 (3.1 - 6.2) | 4.3 (3.2 - 5.1) | 3.7 (3.0 - 5.1) | 3.4 (2.8 - 4.6) | 0.1945 | 0.9798* |
| Peak Horizontal Velocity (mm $s^{-1}$) | 108.8 (72.7 - 138.8) | 112.6 (61.2 - 174.5) | 86.8 (58.6 - 107.5) | 78.7 (67.8 - 149.1) | 0.2712 | 0.8224 |
| Volume Transited ($mm^3$) | 53,786 (20,550 - 95,664) | 65,076 (33,646 - 125,970) | 53,314 (30,734 - 103,950) | 46,406 (22,078 - 118,882) | 0.7416 | 0.3207 |
| Average Turn Angle (degrees) | 56.53 (48.84 - 64.54) | 53.49 (48.45 - 62.04) | 52.05 (45.92 - 60.00) | 52.30 (43.64 - 63.71) | 0.4334 | 0.7863 |
| Average Tortuosity | 3.43 (3.00 - 4.79) | 3.46 (2.97 - 4.35) | 3.39 (2.92 - 4.51) | 3.63 (3.07 - 5.19) | 0.6730 | 0.4065 |

953
954

**Table 5** Variance and coefficient of variation (CV) both per $CO_2$ treatment and overall for all of the 3D arena metrics. $R^2$ are of fits of linear trend lines ($p > 0.05$ for all regressions)

| 3D Metric | | 400 ppm | 1000 ppm | 1600 ppm | 2200 ppm | $R^2$ | Overall |
|---|---|---|---|---|---|---|---|
| 3D Top (% Frames) | $\sigma^2$ | 0.1251 | 0.1007 | 0.0793 | 0.1162 | 0.0956 | 0.1073 |
| | CV | 0.473 | 0.440 | 0.352 | 0.503 | 0.0000 | 0.443 |
| 3D Mid (% Frames) | $\sigma^2$ | 0.0114 | 0.0210 | 0.0106 | 0.0131 | 0.0196 | 0.0143 |
| | CV | 1.48 | 1.16 | 1.22 | 1.09 | 0.7038 | 1.26 |
| 3D Bottom (% Frames) | $\sigma^2$ | 0.1107 | 0.0592 | 0.0585 | 0.1059 | 0.0048 | 0.0852 |
| | CV | 1.85 | 1.59 | 2.10 | 1.50 | 0.0637 | 1.77 |
| Ethology (% Active) | $\sigma^2$ | 593 | 597 | 910 | 590 | 0.0607 | 685 |
| | CV | 0.284 | 0.291 | 0.393 | 0.303 | 0.1615 | 0.321 |
| Total Distance (mm) | $\sigma^2$ | 99,095 | 58,994 | 65,760 | 106,467 | 0.0248 | 87,981 |
| | CV | 0.265 | 0.241 | 0.240 | 0.314 | 0.2961 | 0.275 |
| Average Velocity (mm $s^{-1}$) | $\sigma^2$ | 6.81 | 4.10 | 4.56 | 7.39 | 0.0305 | 6.08 |
| | CV | 0.264 | 0.241 | 0.240 | 0.314 | 0.3072 | 0.275 |
| Peak Velocity (mm $s^{-1}$) | $\sigma^2$ | 95,801 | 192,554 | 51,533 | 341,842 | 0.3596 | 177,644 |
| | CV | 1.20 | 1.56 | 1.33 | 1.89 | 0.3072 | 1.64 |
| Average Jet Velocity (mm $s^{-1}$) | $\sigma^2$ | 14.74 | 11.34 | 16.80 | 25.37 | 0.6506 | 17.99 |
| | CV | 0.221 | 0.221 | 0.258 | 0.314 | 0.8647 | 0.262 |
| Jetting Rate (Jets $s^{-1}$) | $\sigma^2$ | 0.1553 | 0.1556 | 0.0806 | 0.2751 | 0.2083 | 0.1745 |
| | CV | 0.145 | 0.150 | 0.106 | 0.208 | 0.1974 | 0.158 |
| Average Vertical Velocity (mm $s^{-1}$) | $\sigma^2$ | 0.067 | 0.158 | 0.102 | 0.126 | 0.1664 | 0.116 |
| | CV | 9.63 | 6.80 | 2.24 | 5.65 | 0.4854 | 4.61 |
| Average Positive Vertical Velocity (mm $s^{-1}$) | $\sigma^2$ | 4.87 | 5.19 | 3.15 | 4.75 | 0.1147 | 4.89 |
| | CV | 0.232 | 0.293 | 0.207 | 0.260 | 0.0001 | 0.258 |
| Peak Vertical Velocity (mm $s^{-1}$) | $\sigma^2$ | 13,692 | 45,967 | 4,545 | 4,056 | 0.2109 | 17,112 |
| | CV | 0.823 | 1.48 | 0.645 | 0.626 | 0.2097 | 1.07 |
| Average Negative Vertical Velocity (mm $s^{-1}$) | $\sigma^2$ | 2.02 | 1.65 | 1.50 | 2.22 | 0.0338 | 2.02 |
| | CV | 0.248 | 0.280 | 0.235 | 0.288 | 0.1519 | 0.274 |
| Minimum Vertical Velocity (mm $s^{-1}$) | $\sigma^2$ | 14,914 | 48,003 | 4,191 | 179,322 | 0.5174 | 65,185 |
| | CV | 0.988 | 1.73 | 0.718 | 2.68 | 0.3575 | 2.04 |
| Average Horizontal Velocity (mm $s^{-1}$) | $\sigma^2$ | 4.30 | 2.86 | 3.29 | 4.57 | 0.0389 | 3.86 |
| | CV | 0.429 | 0.378 | 0.414 | 0.523 | 0.4426 | 0.442 |
| Peak Horizontal Velocity (mm $s^{-1}$) | $\sigma^2$ | 94,830 | 158,355 | 49,637 | 185,639 | 0.1181 | 125,379 |
| | CV | 1.44 | 1.72 | 1.68 | 1.91 | 0.8284 | 1.76 |
| Volume Transited ($mm^3$) | $\sigma^2$ | $2.86 \times 10^9$ | $4.39 \times 10^9$ | $4.56 \times 10^9$ | $7.71 \times 10^9$ | 0.8710 | $5.06 \times 10^9$ |

This is a post-peer-review, pre-copyedit version of an article published in Hydrobiologia. The final authenticated version is available online at: http://dx.doi.org/10.1007/s10750-017-3342-9

| | | | | | | | |
|---|---|---|---|---|---|---|---|
| | CV | 0.820 | 0.785 | 0.919 | 1.04 | 0.8015 | 0.918 |
| Average Turn Angle (degrees) | $\sigma^2$ | 238.7 | 181.8 | 158.3 | 241.7 | 0.0020 | 211.0 |
| | CV | 0.262 | 0.248 | 0.236 | 0.281 | 0.0890 | 0.261 |
| Average Tortuosity | $\sigma^2$ | 33.51 | 3.18 | 3.59 | 37.56 | 0.0076 | 20.20 |
| | CV | 1.18 | 0.430 | 0.478 | 1.09 | 0.0054 | 0.959 |

955
956

**Table 6** Significant Dunn's posthoc test statistics for differences between $CO_2$ treatments in 3D metrics, $Q_{crit} = 2.631$

| Metric: Treatment | 400 ppm | 1000 ppm | 1600 ppm | 2200 ppm |
|---|---|---|---|---|
| Total Distance (mm): 400 ppm | - | 2.710 | - | - |
| Average Velocity (mm $s^{-1}$): 400 ppm | - | 2.700 | - | - |
| Average Positive Vertical Velocity (mm $s^{-1}$): 400 ppm | - | 3.200 | - | - |
| Average Negative Vertical Velocity (mm $s^{-1}$): 400 ppm | - | 3.741 | - | - |

957

958 Figure Captions

959 **Fig. 1** (A) The set-up for 3D behavior recording placed inside of the tarp-covered photobox
960 showing the wooden frame used to mount the top-facing video camera, the 3D arena in center,
961 with ruler attached for scale, flanked by LED panels on each side, and the front facing video
962 camera. (B) A schematic of the arena set-up showing relative placement of the arena, cameras,
963 and lights. Solid lines indicate seawater volume, while dotted lines indicate arena volume (not to
964 scale, see supplementary Fig. S2). The accompanying model system for the side view (C) and
965 top view (D) to correct positional data for the effect of diminishing axes frames
966
967 **Fig. 2** The proportion of paralarval time spent in the top depth bin in the 2D arena of Experiment
968 1 across $CO_2$ treatments from trials in 2013 (A), 2014 (B), and all trials compiled (C). Dotted
969 circles denote medians and plus signs denote outliers. Lower case letters denote statistical groups
970
971 **Fig. 3** (A) Vertical swimming profile for an ambient (400 ppm) *D. pealeii* paralarvae (individual
972 69_69_08_02) showing depth (blue), vertical velocity (red), and vertical acceleration (gray) over
973 the entire 120-second recording period. (B) A ten-second slice of the swimming profile in A,
974 from 20 seconds to 30 seconds in the video, shows the paralarvae made "hop and sink" jets
975 during descent, rapid ascent, and slow ascent. The velocity peaks represent individual vertical
976 jets
977
978 **Fig. 4** (A) Three-dimensional track of a swimming path for an ambient (400 ppm) *D. pealeii*
979 paralarvae (individual 69_69_08_02). The front of the arena, which the side camera was pointed
980 at, was the right axis face. (B) Three-dimensional polygon of volume transited by the paralarvae
981 during recording. (C) Tortuosity of path traversed by the paralarvae sampled on a sliding frame
982 of one-second path segments. (D) Turning angles along paralarval path, sampled at sequential
983 vectors of one-second path segments
984
985 **Fig. 5** (A) Three-dimensional velocity averaged in ten-second bins across the 120-second
986 recording period. Each line represents an individual paralarvae, with line color denoting their
987 $CO_2$ treatment (400 ppm, blue; 1000 ppm, green; 1600 ppm, orange; 2200 ppm, red). The thick
988 lines represent the median values for all individuals compiled per each $CO_2$ treatment. Although

This is a post-peer-review, pre-copyedit version of an article published in Hydrobiologia. The final authenticated version is available online at: http://dx.doi.org/10.1007/s10750-017-3342-9

989 individual are remarkably variable over their path and overall, the median lines demonstrate both
990 the decrease in velocity at exposures above 400 ppm and the consistency in overall behavior over
991 time in the arena. (B) The time-binned average velocity data (lines denote medians, colors denote
992 $CO_2$ treatment as in A) reinforces the high variability in the whisker length and number of
993 outliers (represented as plus signs), and shows both consistently higher velocities in the 400 ppm
994 treatment and broadly consistent median values within $CO_2$ treatments across the recording time

This is a post-peer-review, pre-copyedit version of an article published in Hydrobiologia. The final authenticated version is available online at: http://dx.doi.org/10.1007/s10750-017-3342-9

Fig. 1

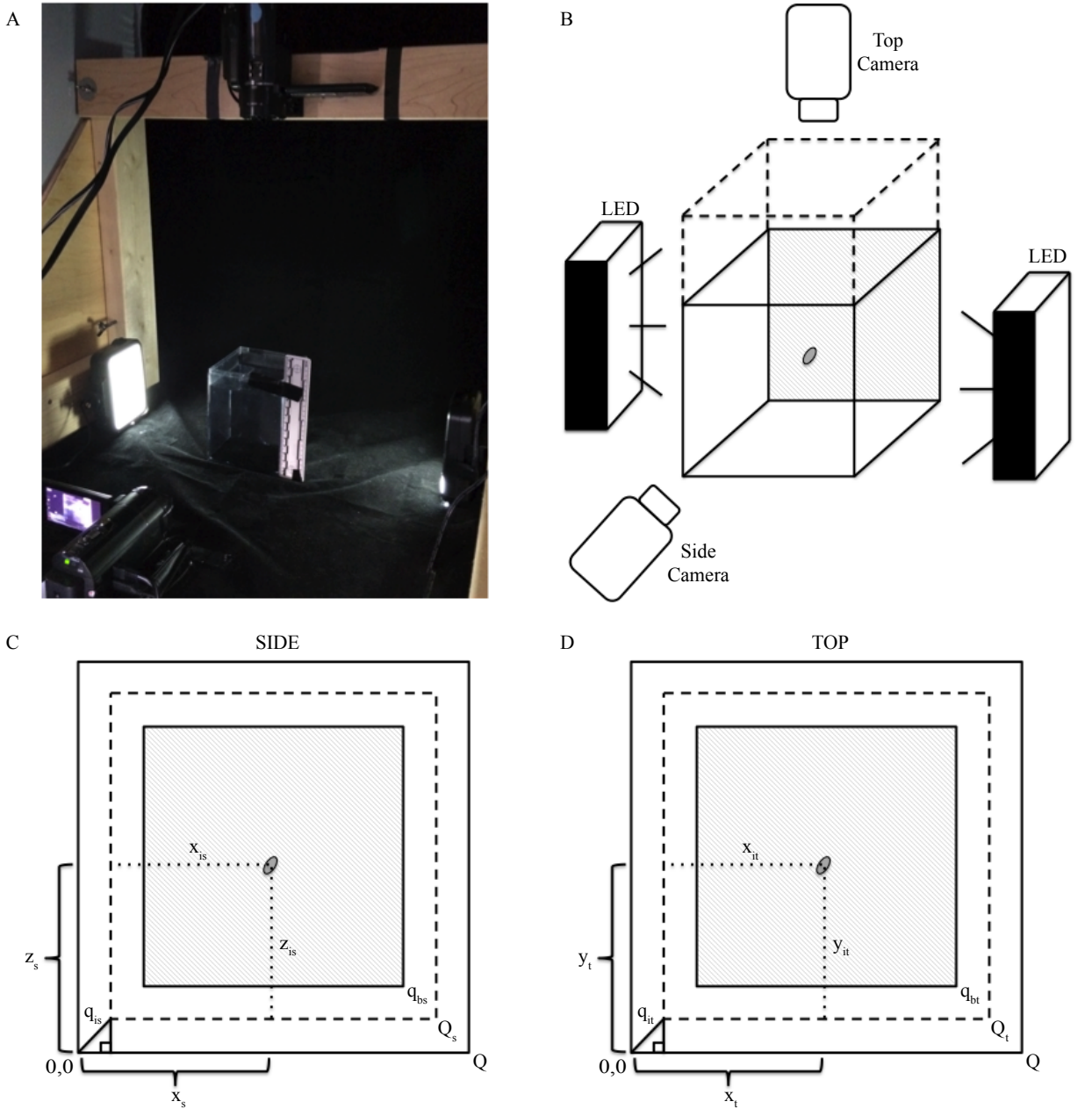
A
B
Top
Camera
LED
LED
Side
Camera
C
SIDE
$x_{is}$
$z_{is}$
$z_s$
$q_{bs}$
$q_{is}$
$Q_s$
0,0
Q
$x_s$
D
TOP
$x_{it}$
$y_{it}$
$y_t$
$q_{bt}$
$q_{it}$
$Q_t$
0,0
Q
$x_t$

Fig. 2

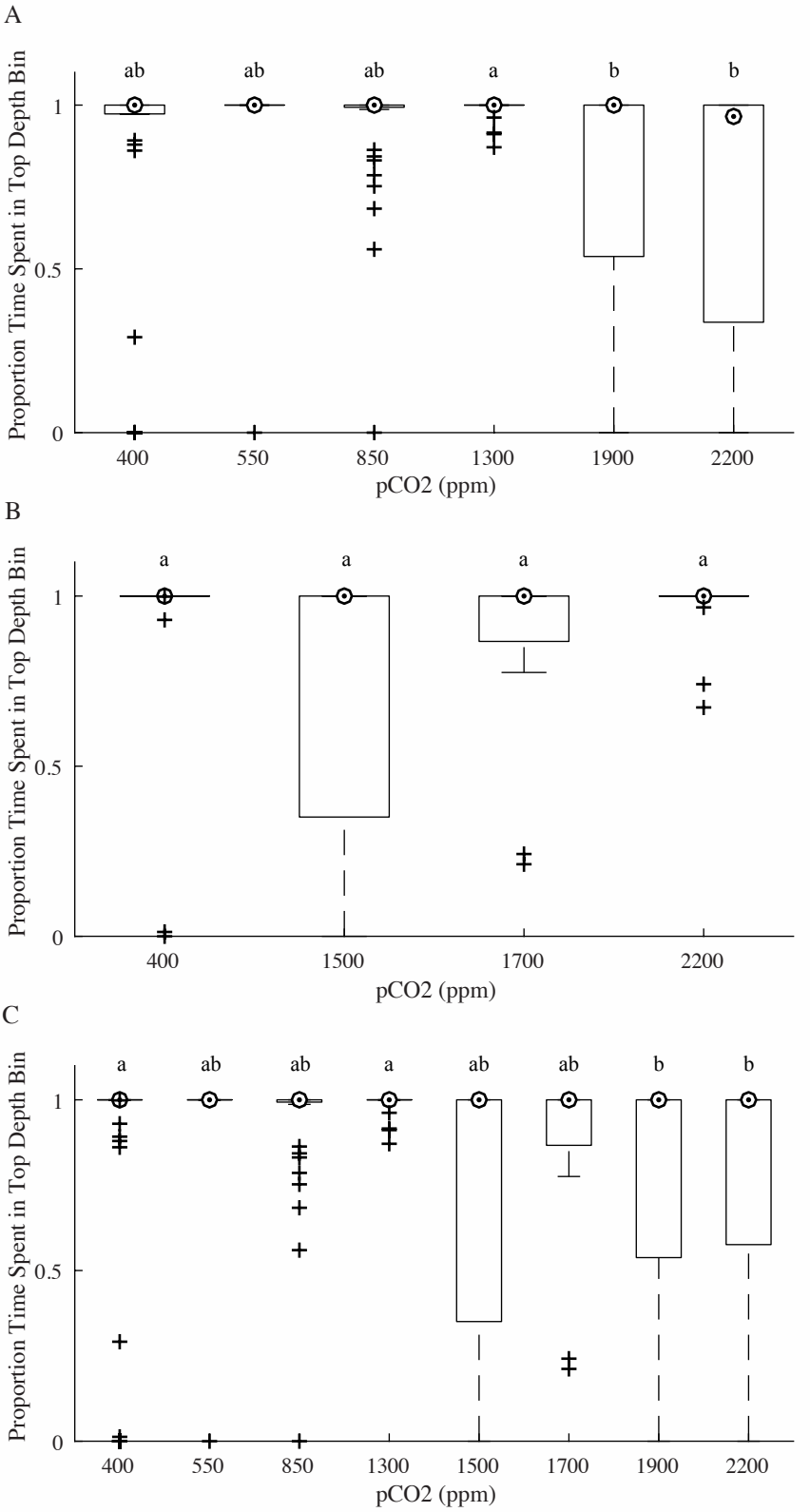
A
ab
ab
ab
a
b
b
1
0.5
0
Proportion Time Spent in Top Depth Bin
400
550
850
1300
1900
2200
pCO2 (ppm)
B
a
a
a
a
1
0.5
0
Proportion Time Spent in Top Depth Bin
400
1500
1700
2200
pCO2 (ppm)
C
a
ab
ab
a
ab
ab
b
b
1
0.5
0
Proportion Time Spent in Top Depth Bin
400
550
850
1300
1500
1700
1900
2200
pCO2 (ppm)

Fig. 3

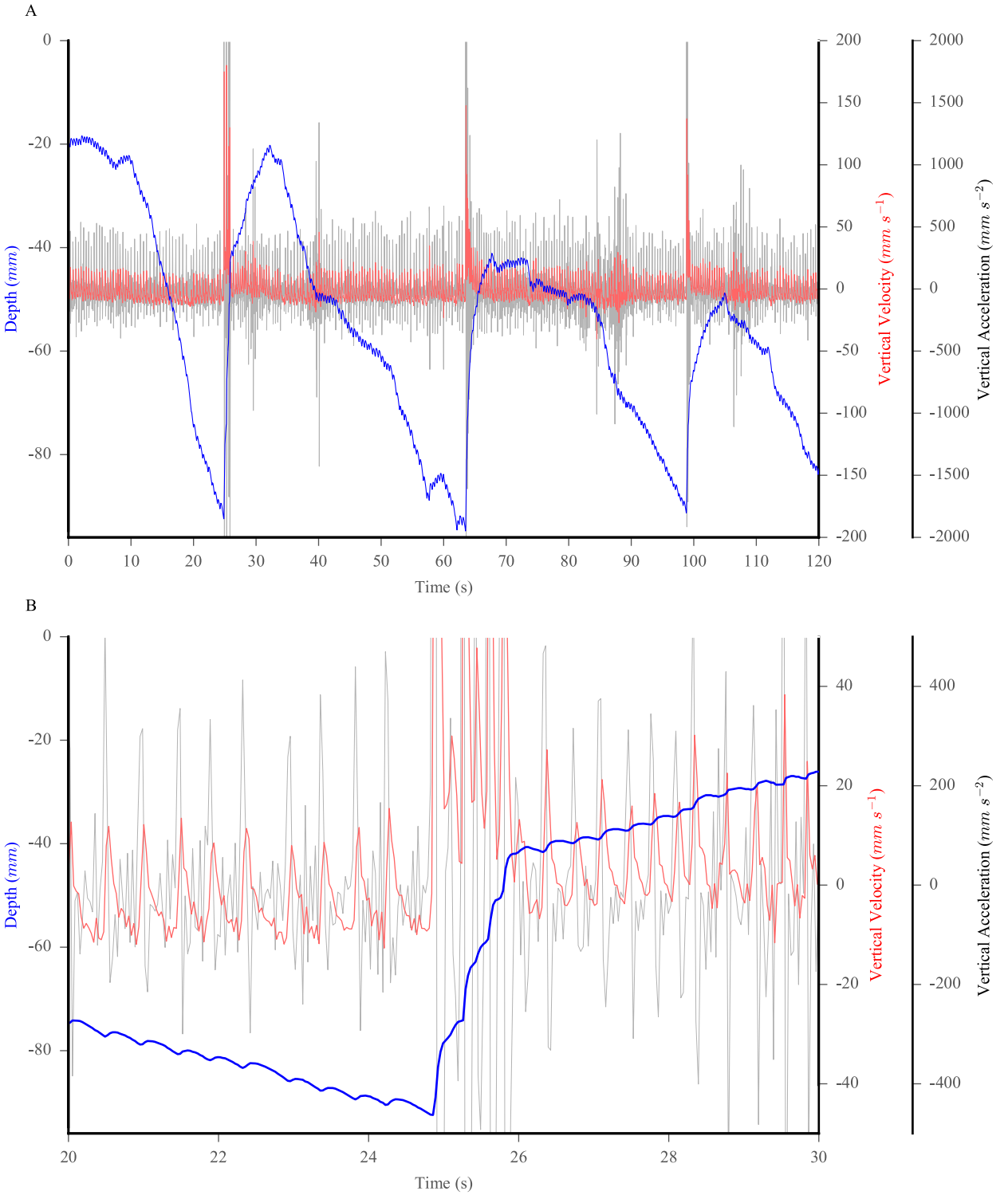
A
Depth (mm)
Vertical Velocity (mm s⁻¹)
Vertical Acceleration (mm s⁻²)
Time (s)
B
Depth (mm)
Vertical Velocity (mm s⁻¹)
Vertical Acceleration (mm s⁻²)
Time (s)

Fig. 4

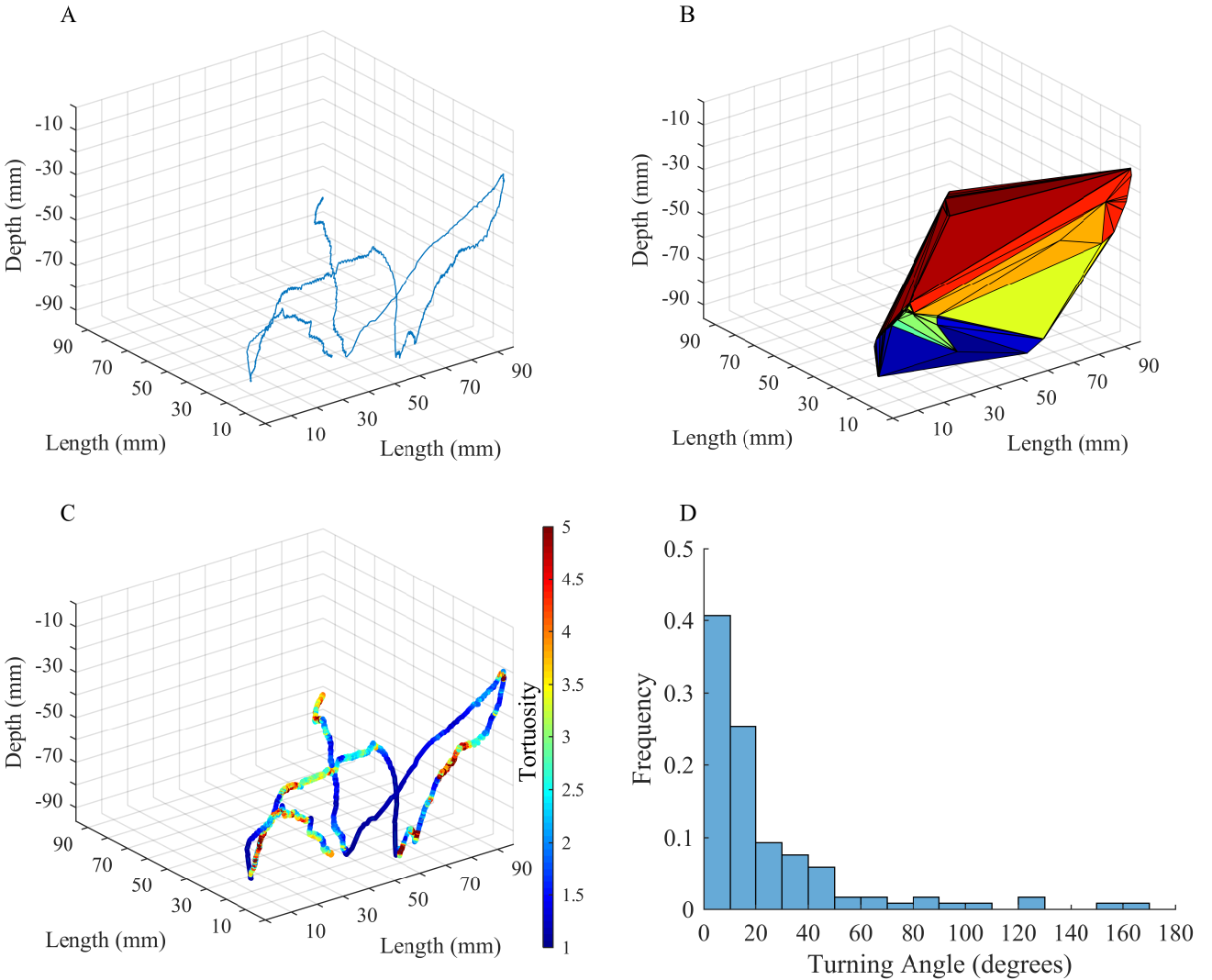
A
B
C
D
Depth (mm)
-10
-30
-50
-70
-90
Length (mm)
90
70
50
30
10
Tortuosity
5
4.5
4
3.5
3
2.5
2
1.5
1
Frequency
0.5
0.4
0.3
0.2
0.1
0
0
20
40
60
80
100
120
140
160
180
Turning Angle (degrees)

Fig. 5

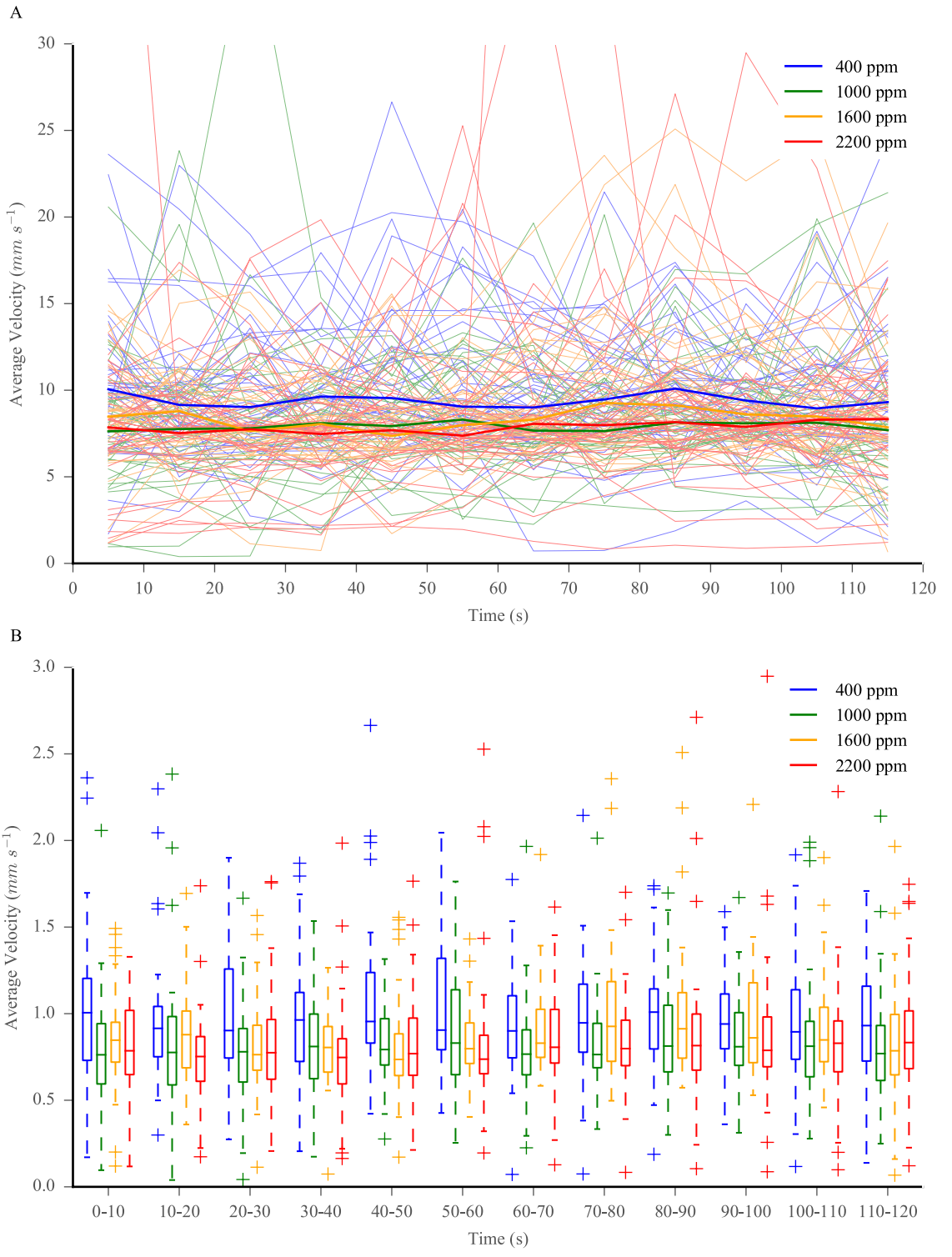
A
400 ppm
1000 ppm
1600 ppm
2200 ppm
Average Velocity ($mm\ s^{-1}$)
Time (s)
B
400 ppm
1000 ppm
1600 ppm
2200 ppm
Average Velocity ($mm\ s^{-1}$)
0-10
10-20
20-30
30-40
40-50
50-60
60-70
70-80
80-90
90-100
100-110
110-120
Time (s)